

MSc Project - Modelling a Double-Barred Galaxy as a Double Binary

Howard Kinsman

August 18, 2017

Abstract

TODO

1 Introduction

1.1 Double-Barred Galaxies

Double-barred galaxies, where a smaller inner bar is nested inside a larger outer bar, were first observed in 1975 by de Vaucouleurs (de Vaucouleurs, 1975), however it was only in the 1990s that double-barred galaxies were recognised as being a distinct category of galaxies. The current estimates of double-barred galaxy frequencies are $\approx 30\%$ of barred galaxies and $\approx 20\%$ of all galaxies (Erwin, 2003). Erwin (2011) surveyed 38 barred galaxies and found a total of 10 double-barred galaxies with no preference for Hubble type. They found that inner bars were about 12% the size of the outer bars with semi-major axes from $\approx 250\text{pc}$ to 1 kpc. Secondary bars probably rotate independently of, but in the same direction as their associated primary bars Erwin (2011). Erwin and Sparke (2002) believe that inner bars probably rotate independently of their outer bars and suggest that they are relatively long-lived structures. Inner bar size has been found to correlate slightly with outer bar size (Erwin, 2003). The median size ratio is ≈ 0.12 with an upper limit of ≈ 0.25 which is consistent with the theory that inner bars cannot be too large without disrupting the orbit of the outer bar.

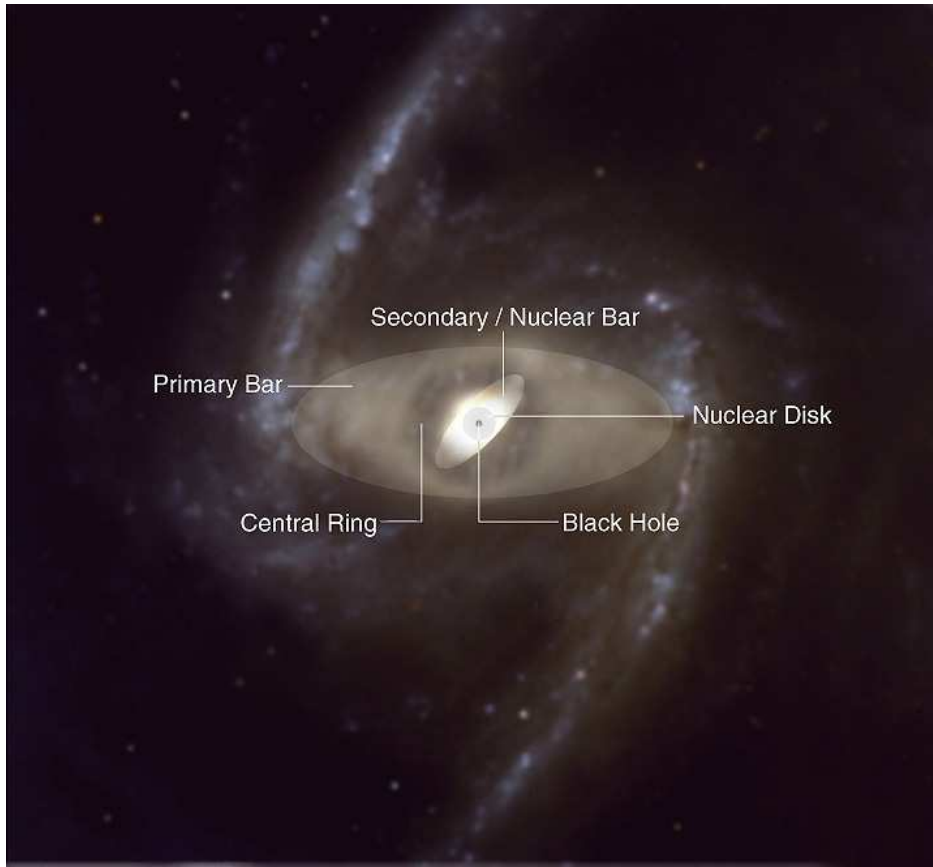


Figure 1: This is a schematic drawing of the various components of a double-barred galaxy. Credit: ESO

It has been suggested that nested bars may provide a mechanism for fueling active galactic nuclei (Shlosman et. al., 1989) however more recently (Erwin, 2003) believe that inner bars only play a minor role in this activity. (Erwin and Sparke, 2002) compared single and double-barred galaxies and found that there was no significant difference in nuclear activity. To investigate this theory further Lorenzo-Caceres et. al. (2002) carried out a study of NGC 357. This study aimed to present the first detailed morphological, kinematical and stellar population analysis of the bulge, inner and outer bars of a double-barred galaxy. They concluded that the bulge and inner bar show similar stellar population properties whilst the outer bar was less metal-rich. This result implied that, for the case of NGC 357, the outer bar was formed in a shorter timescale than the inner structures and so disagrees with traditional idea that gas flown along the outer structure triggers star formation causing the formation of the inner structure. This was strengthened by a further study of four double-barred galaxies by Lorenzo-Caceres et. al. (2013)

where they concluded that the stellar populations of inner bars are younger and more metal-rich than the outer bars. This suggests that at present inner bars play a moderate or even minor role in the morphological evolution of double-barred galaxies (Lorenzo-Caceres et. al., 2013).

Through the use of computer modeeling Saha and Maciejewski (2013) showed that double bars can form without gas in a dark matter dominated halo. They produced a model where the inner bar was rotating at almost as slowly as the outer bar. The route to the formation of double bars maybe very different to that of a single bar.

1.2 N-Body Simulations and the Four-Body Problem

Studies of three or more bodies interacting gravitationally dates back to the time of Newton. However it is only with the widespread use of computers that orbits of more than three bodies have been extensively studied. Today N-body simulations are an essential tool in the study of solar system dynamics and galactic dynamics. The orbit-integration problems we have to address vary in complexity from following a single particle in a given, smooth galactic potential, to tens of thousands of interacting stars in a globular cluster, to billions of dark-matter particles in a simulation of cosmological clustering (Binney and Tremaine, 2008). Celestial mechanics during the preceding centuries has mainly focussed on the three body problem due to the complexities involved in adding more bodies. It is estimated that within the Milky Way approximately two thirds of all stars exist in binary systems and a further one fifth of these are in triple systems whilst a further fifth still exist in systems with more than three bodies (Steves and Roy, 1998). Steves and Roy (1998) estimate that $\approx 2 \times 10^9$ quadruple systems exist in the Milky Way galaxy. They found that quadruple systems exist in two forms: a double binary or linear.

The classical equations of motion for an N-body problem are:

$$m_i \ddot{\mathbf{r}} = \sum_{i \neq j} \frac{m_i m_j}{r_{ij}^3} \mathbf{r}_{ij} \quad i = 1, 2, 3, \dots \quad (1)$$

where $\mathbf{r}_i = (x_i, y_i)$ and $\mathbf{r}_{ij} = \mathbf{r}_j - \mathbf{r}_i$. The units have been selected so that the gravitational constant (G) is equal to one. In simulations it is natural to choose units where $G = 1$ and the units of length and mass are conventionally chosen so that the total mass of the system is $M = 1$ (Heggie and Hut, 2003).

The four body problem, specifically, has been studied extensively by Steves and Roy (1998). Here they model four equal mass bodies orbiting in circular coplanar orbits. This model they term the Caledonian problem,

because their research is being carried out at Glasgow Caledonian University. Approximately a century ago the Copenhagen problem was studied extensively in Copenhagen which consisted of a three body problem: two equal mass bodies and an infinitesimally small test particle. Szell et. al. (2004) also studied the Caledonian problem and found that the stability of the system is dependent upon a constant termed the Szebehely constant. The Caledonian Symmetric Double Binary Problem (CSDBP) is relevant in studying the stability and evolution of symmetric quadruple stellar clusters and exoplanetary systems of two planets orbiting a binary pair of stars (AlvarezRamirez and Medina, 2014).

Methods for the study of N-body simulations have changed considerably since the advent of computers. In a study of N-body simulations Trenti and Hut (2008) mentions a pioneering attempt by Holmberg in 1941 which used light bulbs and galvanometers to track the evolution of 37 particles. However it wasn't until the early seventies and the advent of computers that this field really got started. Nowadays simulations can up to a million particles (Heggie and Hut, 2003) which is of particular relevance to the study of globular clusters. I refer the reader to Aarseth (2003) for much more detailed explanation of the field of N-body simulations.

1.3 Orbits, Loops, Resonances and Double-Barred Galaxy Simulations

Double-barred galaxy simulations and models have taken many forms. Du et. al. (2015) explored the formation and evolution of double-barred galaxies (which is not very well understood) by showing that a dynamically cool inner disk embedded in a hotter outer disk can generate a secondary bar while the outer disk forms a large-scale primary bar. Maciejewski et. al. (2001) used hydrodynamical simulations to study gas inflow in barred galaxies and the effect this has on secondary bars. They concluded that the secondary bar can prevent, rather than enhance, the inflow. More recently, Debattista and Shen (2007) used collisionless N-body simulations to show that inner bars can form spontaneously without requiring gas. They also found that secondary bars rotate faster than primary bars and that the secondary bars pulsate. This is considered further in the Discussion.

In an attempt to explain the dynamics of the orbits of nested bars Maciejewski and Sparke (1999) introduced the concept of ‘loops’. They wanted to investigate how two independently rotating bars can maintain themselves as gravitating systems. A gravitational potential consisting of two concentric bisymmetric bars that are independently rotating is not stationary in any

reference frame Maciejewski and Sparke (1999). In the potential of a single bar particles would stay on a stable closed periodic orbit but with nested bars orbits will not be closed because the particles would be experience two separate forces. The ‘loop’ therefore was introduced as an extension of the concept of orbit. Particles in a ‘loop’ would return to their original positions every time the bars come back to the same relative orientation (Maciejewski and Sparke, 1999). This lead to the conclusion that loops supporting the inner bar are thicker with parallel bars and thinner with perpendicular bars (Maciejewski, 2008). This also suggests that the two bars do not rotate through each other as rigid bodies but the inner bar should pulsate and that the bars should spend more time nearly orthogonal (Maciejewski, 2008). These predictions were confirmed by (Debattista and Shen, 2007) and (Shen and Debattista, 2008). This was further confirmed by Maciejewski and Small (2010) who found that the inner bar should end well within its corotation radius and that the inner bar extends further out for lower pattern speeds than higher ones; the inner bar pulsates; and that the angular velocity of the inner bar is not uniform and that faster inner bars rotate more coherently.

Wozniak (2015) also carried out double-barred galaxy simulations and achieved long-lived inner bars lasting for up to 7 Gyr. These were N-body/hydrodynamical simulations. They found that the two bar lengths, ratio of pattern speeds, as well as the age of the inner stellar bar populations in the simulations matched well with observations. They concluded that because, unlike previous simulations, there was no overlap between primary bar inner Lindblad resonance (ILR) and the inner bar corotation (CR) or any kind of resonance overlap, then some other kind of mechanism must feed the central waves (Wozniak, 2015). It is suggested that star formation may be responsible for bringing energy into the inner bar.

Garzon (2014) studied the dynamical evolution of two isolated bars, within the same galaxy, under their mutual gravitational interaction. They considered two cases purely analytically: rotation of rigid bodies and rotation of deformable rotation. They found that the bars oscillate in size according to the relative angle between the bars. This is broadly in agreement with (Debattista and Shen, 2007). What follows is an attempt to verify the calculations in (Garzon, 2014) but using a simpler model of a double-barred galaxy using a double binary.

2 Methods

The model was created using OdeInt from Numerical Recipes (Press et. al., 1992). OdeInt was first converted to Fortran 90 for this purpose. Fortran 90 was selected as the language of choice in order to avoid the fixed line limitations of Fortran 77. OdeInt performs integration using the Runge-Kutta method. The Runge-Kutta method is an extension of the Euler method of solving differential equations. However the Euler method is an example of first-order integration whilst Runge-Kutta is second and higher order and so is much more accurate. The OdeInt uses a subroutine called RK4 which utilises fourth-order Runge-Kutta integration. It also uses a technique known as adaptive stepsize. This involves adjusting the size of the integration steps to ensure the same level of accuracy however rapidly the function being integrated changes. Many small steps should tiptoe through treacherous terrain, while a few great strides should speed through smooth uninteresting countryside (Press et. al., 1992).

For a four body problem, Equation 1 results in the following:

$$\ddot{\mathbf{r}}_1 = \frac{m_2 \mathbf{r}_{12}}{r_{12}^3} + \frac{m_3 \mathbf{r}_{13}}{r_{13}^3} + \frac{m_4 \mathbf{r}_{14}}{r_{14}^3} \quad (2)$$

$$\ddot{\mathbf{r}}_2 = \frac{m_1 \mathbf{r}_{21}}{r_{21}^3} + \frac{m_3 \mathbf{r}_{23}}{r_{23}^3} + \frac{m_4 \mathbf{r}_{24}}{r_{24}^3} \quad (3)$$

$$\ddot{\mathbf{r}}_3 = \frac{m_1 \mathbf{r}_{31}}{r_{31}^3} + \frac{m_2 \mathbf{r}_{32}}{r_{32}^3} + \frac{m_4 \mathbf{r}_{34}}{r_{34}^3} \quad (4)$$

$$\ddot{\mathbf{r}}_4 = \frac{m_1 \mathbf{r}_{41}}{r_{41}^3} + \frac{m_2 \mathbf{r}_{42}}{r_{42}^3} + \frac{m_3 \mathbf{r}_{43}}{r_{43}^3} \quad (5)$$

These equations of motion are second-order ordinary differential equations (ODEs) but any second-order ODE can be written as a system of two coupled first-order ODEs. As there are four bodies in the system, and they all have x and y positional components, this gives eight second-order ODEs which leaves us with a total of sixteen simultaneous first-order ODEs to solve. These equations were encoded into Fortran. A full code listing is supplied in a separate file.

2.1 Initial Conditions

As a starting point both the outer binary and inner binary were placed in circular orbits and tested separately and then combined to ensure a stable starting point. The inner binary had an initial negligible mass. The outer binary initial conditions were:

$m1=.5$, $m2=.5$, $x1=-.5$, $x2=.5$, $y1=0$, $y2=0$,
 $vx1=0$, $vx2=0$, $vy1=-.5$, $vy2=.5$

and for the inner binary:

$m3=.001$, $m4=.001$, $x3=-.001$, $x4=.001$, $y3=0$, $y4=0$,
 $vx3=0$, $vx4=0$, $vy3=-.5$, $vy4=.5$

Plots of the two initial binaries are shown in Fig. 2 and 3. The velocity of the inner binary is high and therefore few points are seen in this initial plot.

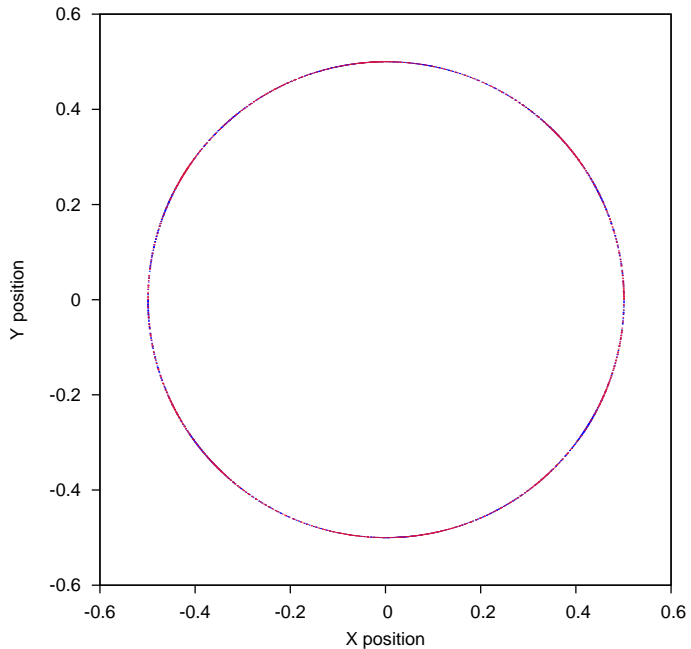


Figure 2: Outer Binary

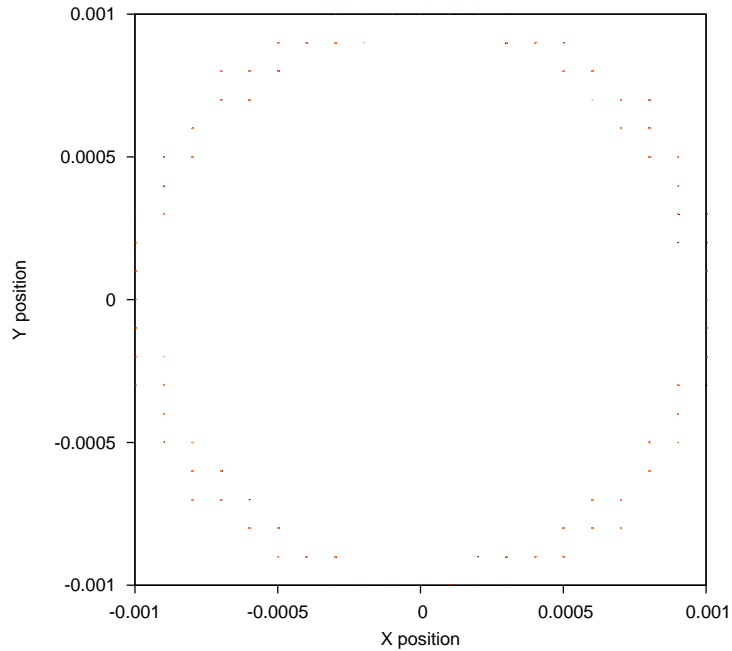


Figure 3: Inner Binary

I then proceeded to perturb the system by gradually increasing the mass of the inner binary. As the system became unstable I compensated for the increasing mass of the inner binary by increasing the velocity of the outer binary and also decreasing the velocity and increasing the binary separation of the inner binary. In many of the configurations the systems were inherently unstable and produced collisions with some or all of the bodies being ejected from the system. These were rejected and only ‘stable’ configurations were considered. Table 1 shows the perturbations made to the system - only the variables in this table changed and all the other initial conditions remained the same.

Table 1: Configurations

Config.	m3	m4	vy1	vy2	x3	x4	vy3	vy4
1	.001	.001	-.5	.5	-.001	.001	-.5	.5
2	.002	.002	-.5	.5	-.001	.001	-.5	.5
3	.003	.003	-.5	.5	-.001	.001	-.5	.5
4	.004	.004	-.5	.5	-.004	.004	-.5	.5
5	.004	.004	-.55	.55	-.004	.004	-.5	.5
6	.004	.004	-.57	.57	-.004	.004	-.5	.5
7	.005	.005	-.58	.58	-.005	.005	-.3	.3
8	.005	.005	-.58	.58	-.005	.005	-.4	.4
9	.005	.005	-.58	.58	-.005	.005	-.35	.35
10	.006	.006	-.6	.6	-.006	.006	-.3	.3
11	.025	.025	-.65	.65	-.02	.02	-.5	.5
12	.025	.025	-.7	.7	-.025	.025	-.5	.5
13	.03	.03	-.7	.7	-.03	.03	-.5	.5
14	.035	.035	-.75	.75	-.04	.04	-.4	.4
15	.04	.04	-.75	.75	-.045	.045	-.4	.4
16	.05	.05	-.75	.75	-.045	.045	-.4	.4
17	.05	.05	-.75	.75	-.05	.05	-.35	.35
18	.05	.05	-.75	.75	-.05	.05	-.3	.3
19	.06	.06	-.8	.8	-.06	.06	-.25	.25
20	.08	.08	-.9	.9	-.08	.08	-.15	.15
21	.09	.09	-.95	.95	-.09	.09	-.1	.1
22	.1	.1	-1	1	-.1	.1	-.05	.05
23	.1	.1	-1	1	-.1	.1	-.04	.04
24	.1	.1	-1	1	-.1	.1	-.03	.03
25	.1	.1	-1	1	-.1	.1	-.02	.02
26	.12	.12	-1.05	1.05	-.11	.11	-.015	.015
27	.12	.12	-1.1	1.1	-.11	.11	-.015	.015
28	.12	.12	-1.1	1.1	-.115	.115	-.015	.015
29	.12	.12	-1.1	1.1	-.12	.12	-.015	.015
30	.1	.1	-1	1	-.1	.1	-.1	.1
31	.1	.1	-1	1	-.102	.102	-.1	.1
31	.1	.1	-1	1	-.1021	.1021	-.1	.1

3 Results

As can be seen from Fig. 4 even a negligible mass inner binary causes the outer binary to begin to separate and become less tightly bound. Figures Fig. 4 to 67 show plots of the double binary using the parameters given in Table 1. In many cases the inner binary is only visible as a point at the centre of the outer binary. As the mass of the inner binary increased the system became increasingly unstable and the effect on the outer binary became more pronounced. Even the ‘stable’ configurations listed in Table 1 hold for only a few orbits.

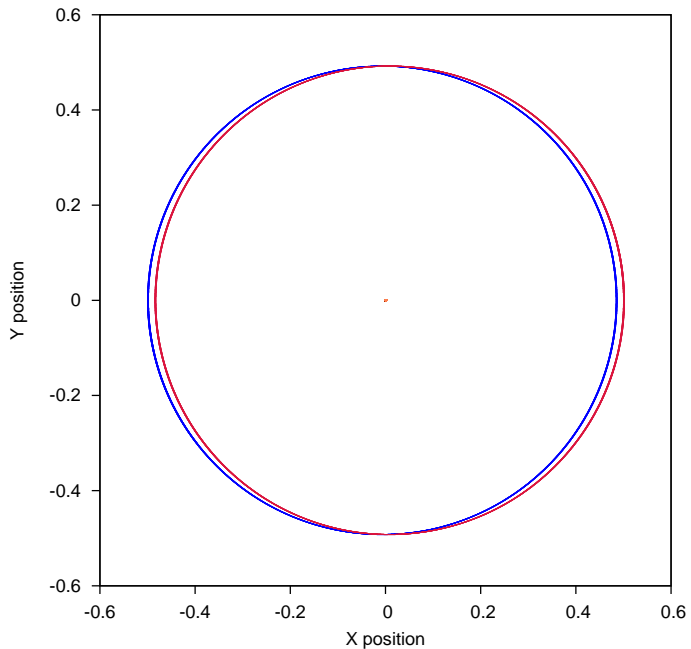


Figure 4: Configuration 1

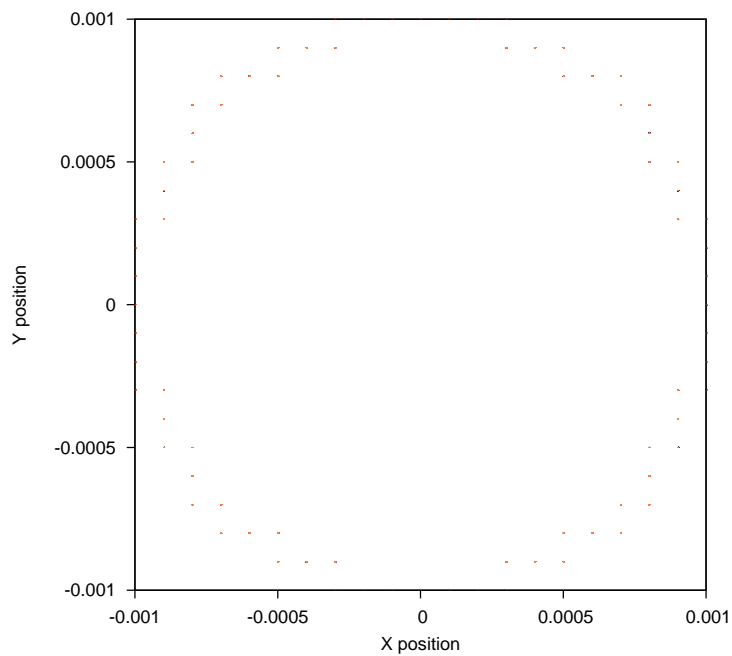


Figure 5: Configuration 1 - Inner Bar

Figs. 4 and 5 show the initial orbits when the circular inner binary is placed within the outer binary.

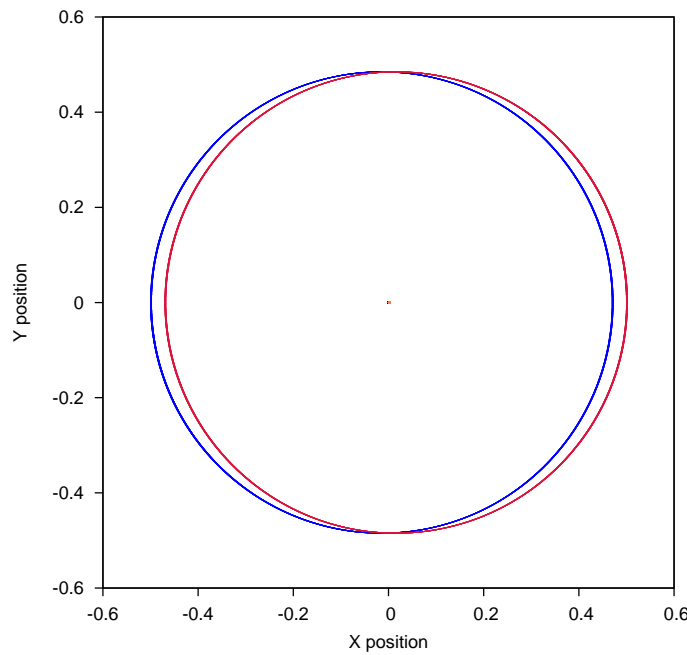


Figure 6: Configuration 2

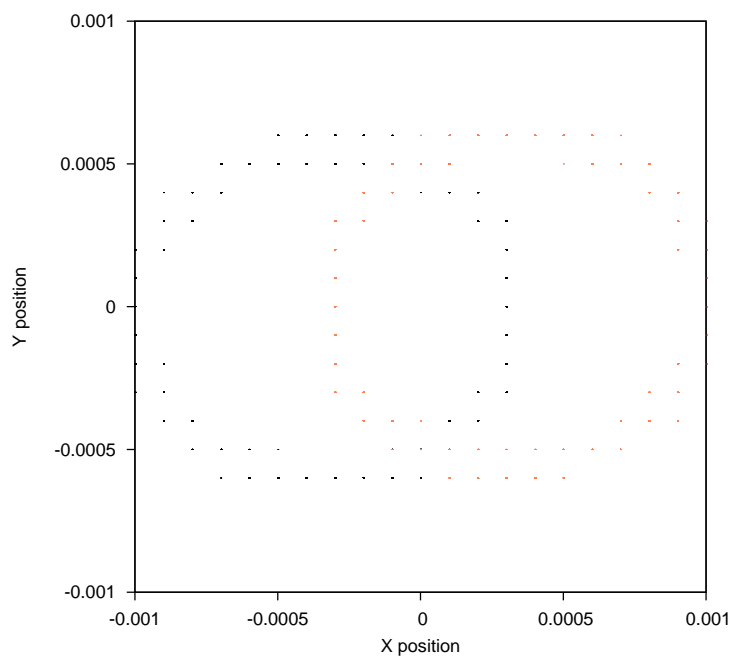


Figure 7: Configuration 2 - Inner Bar

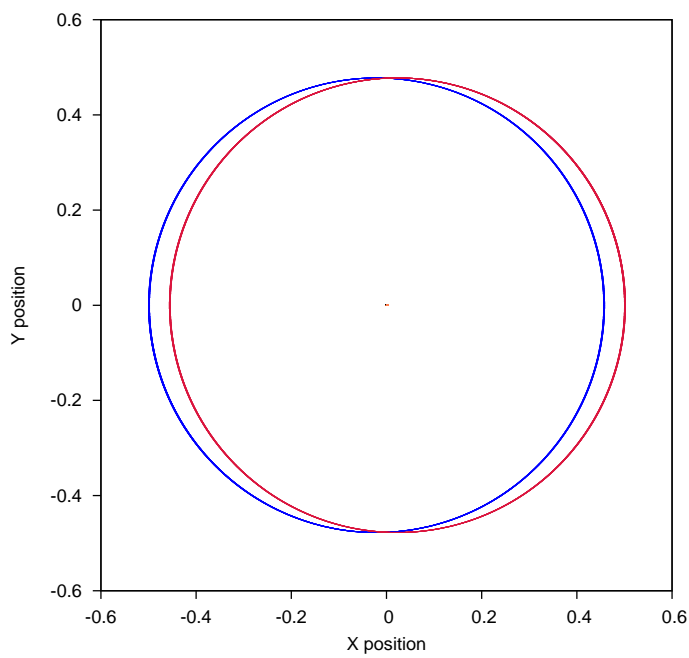


Figure 8: Configuration 3

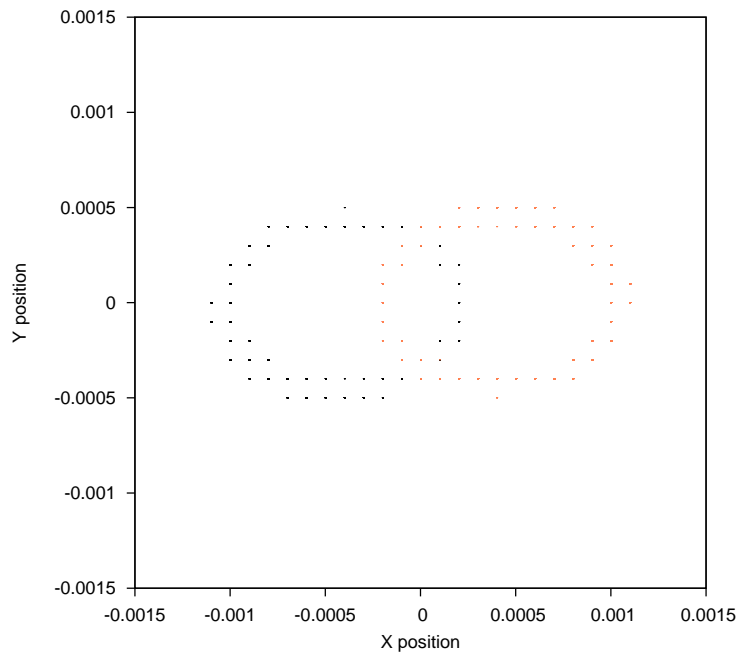


Figure 9: Configuration 3 - Inner Bar

Figs. 6 to 9 show plots where just the mass of the inner binary has been gradually increased. Nothing else was changed. By Fig. 9, the inner binary can clearly be seen to be pulled apart by the gravitational affect of the outer binary.

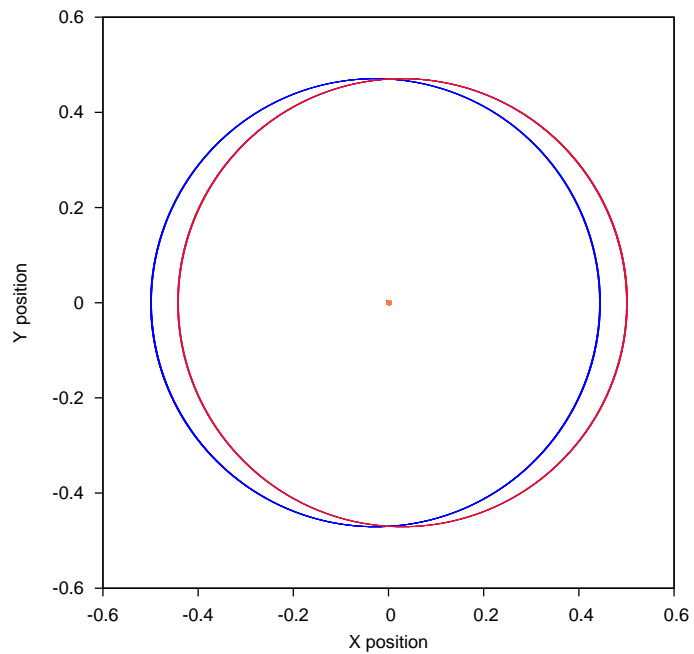


Figure 10: Configuration 4

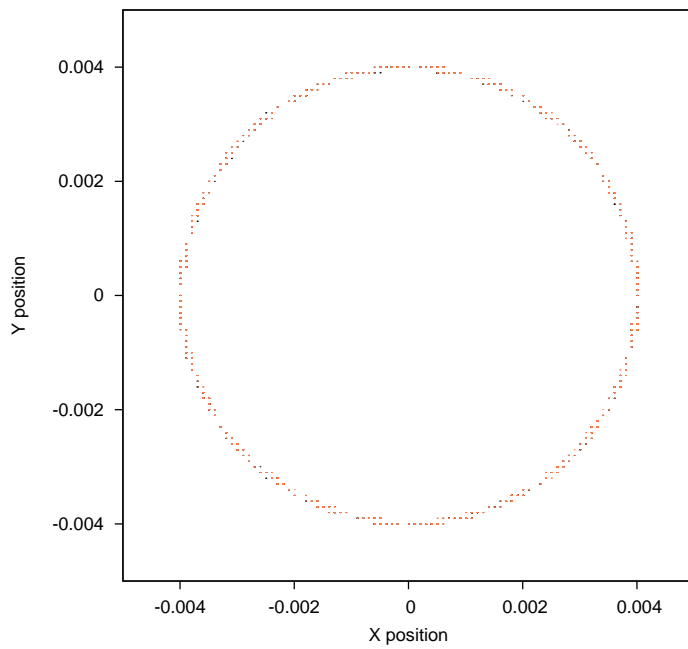


Figure 11: Configuration 4 - Inner Bar

To counteract the effect of the increased mass of the inner binary in Figs. 10 and 11 the initial separation of the inner binary has been increased.

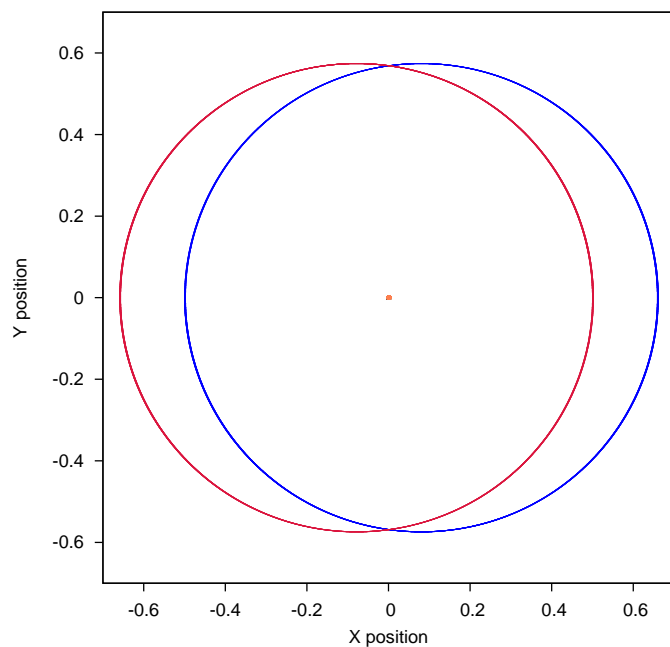


Figure 12: Configuration 5

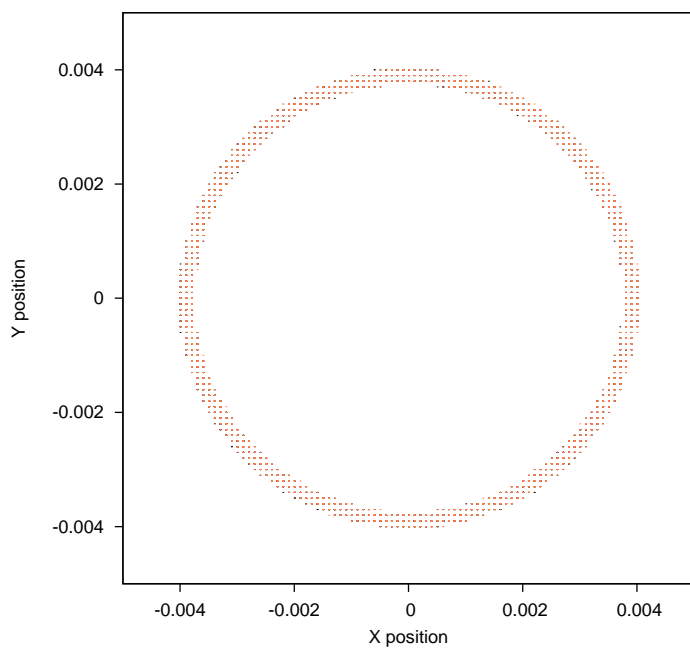


Figure 13: Configuration 5 - Inner Bar

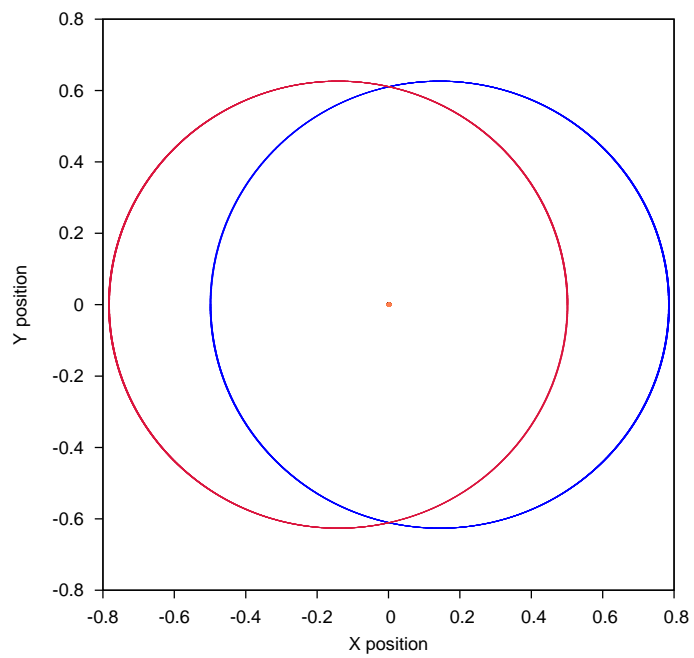


Figure 14: Configuration 6

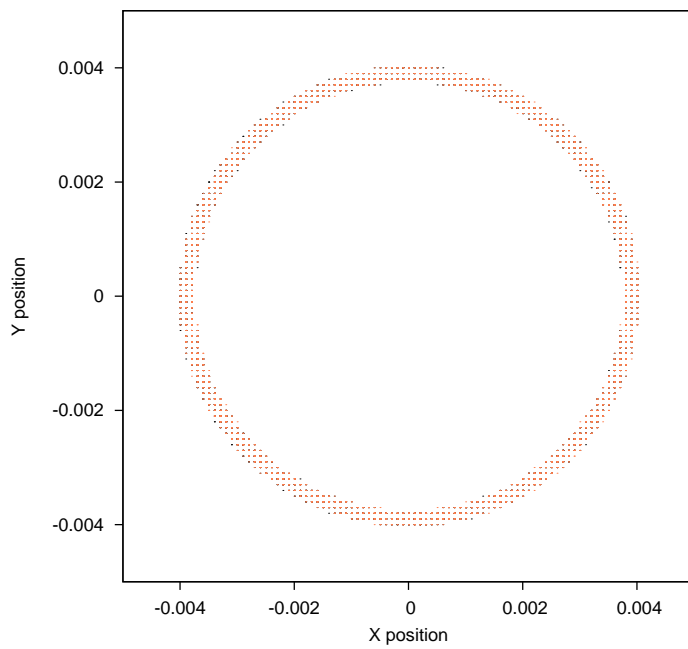


Figure 15: Configuration 6 - Inner Bar

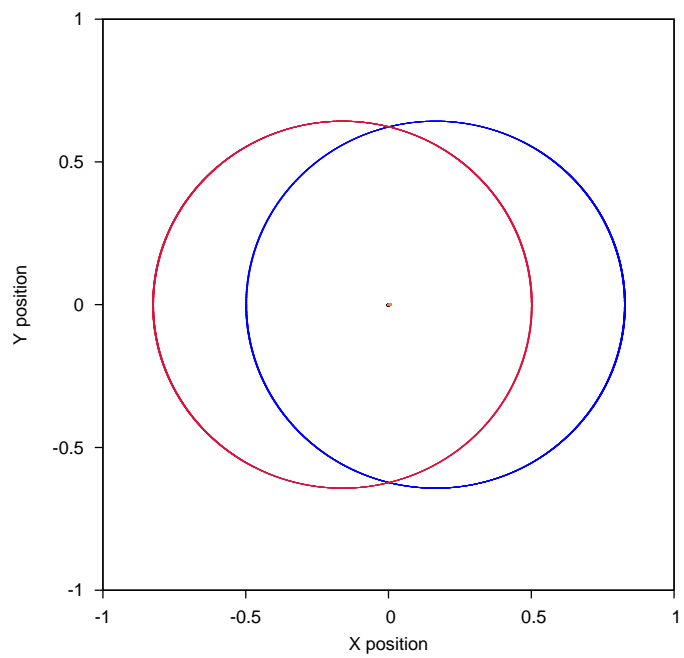


Figure 16: Configuration 7

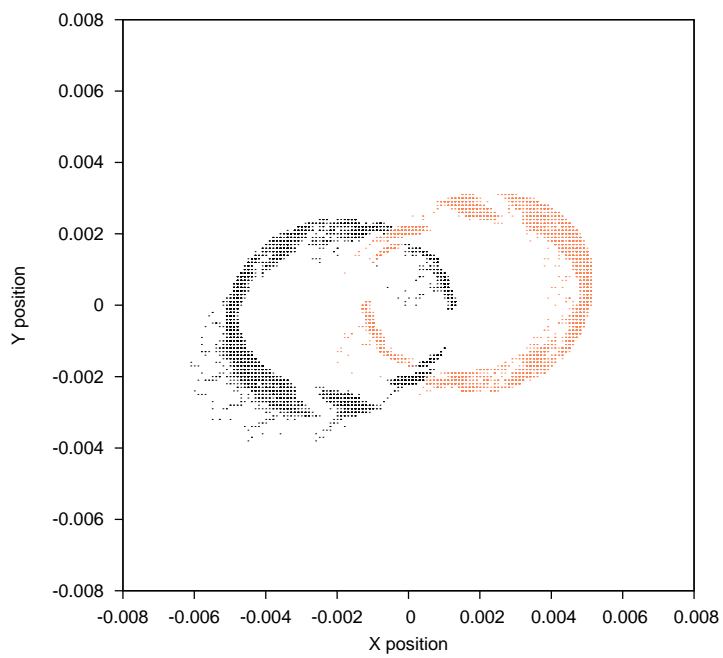


Figure 17: Configuration 7 - Inner Bar

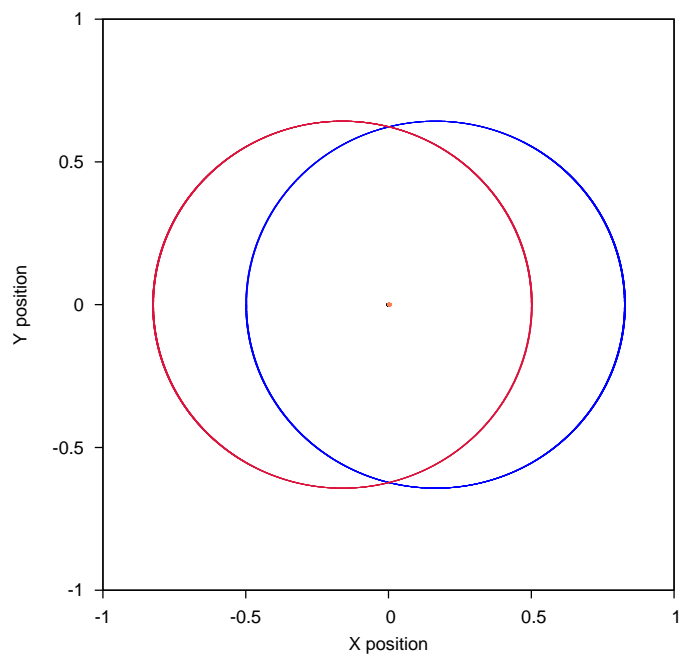


Figure 18: Configuration 8

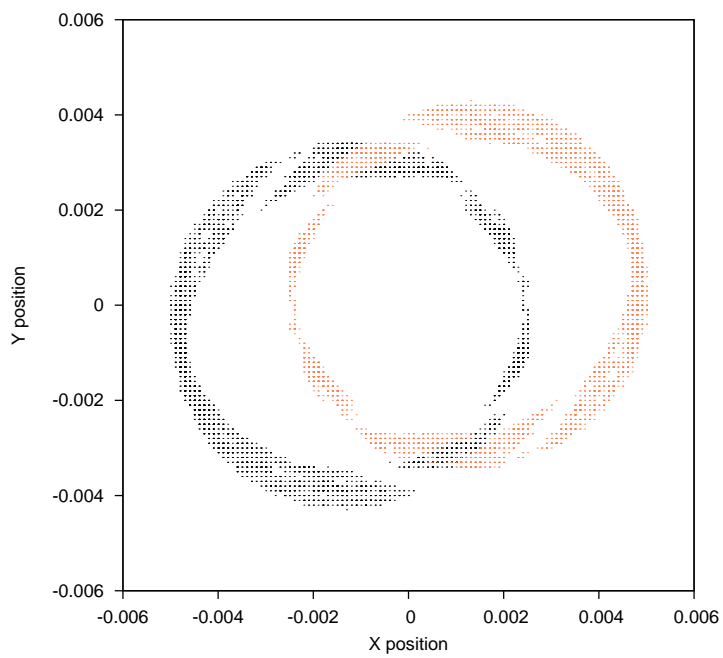


Figure 19: Configuration 8 - Inner Bar

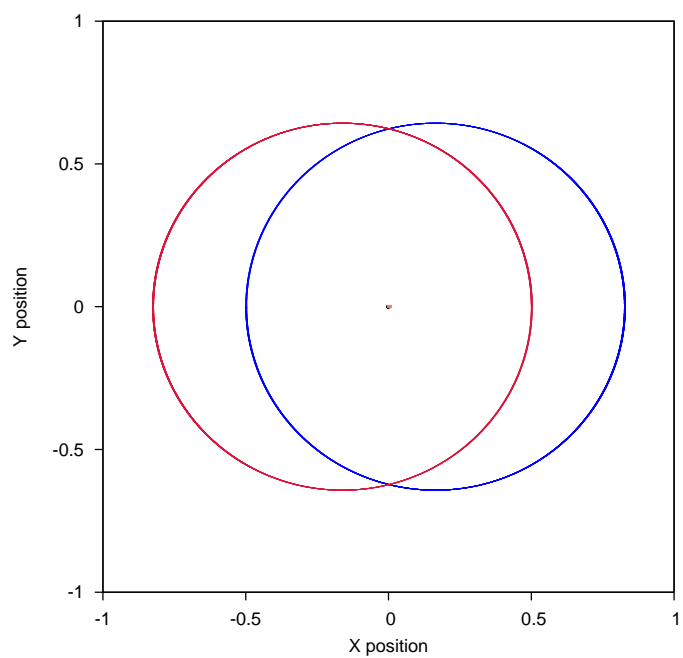


Figure 20: Configuration 9

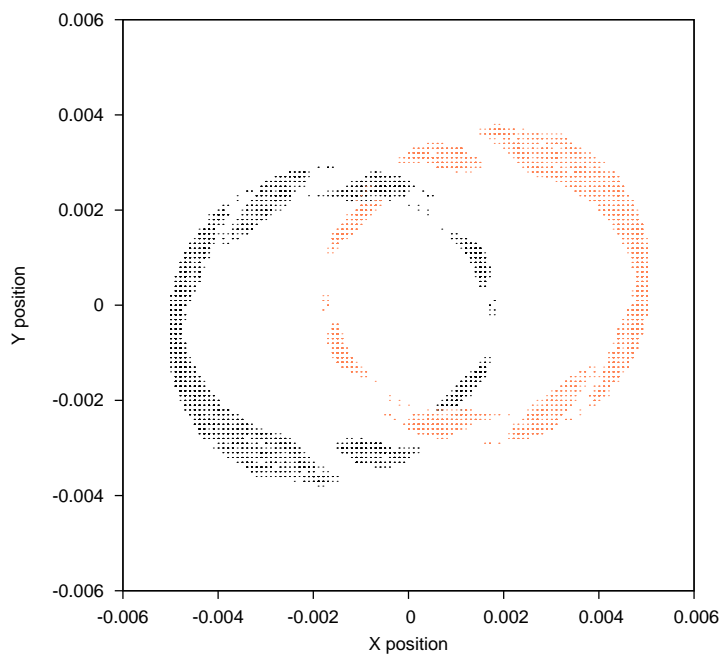


Figure 21: Configuration 9 - Inner Bar

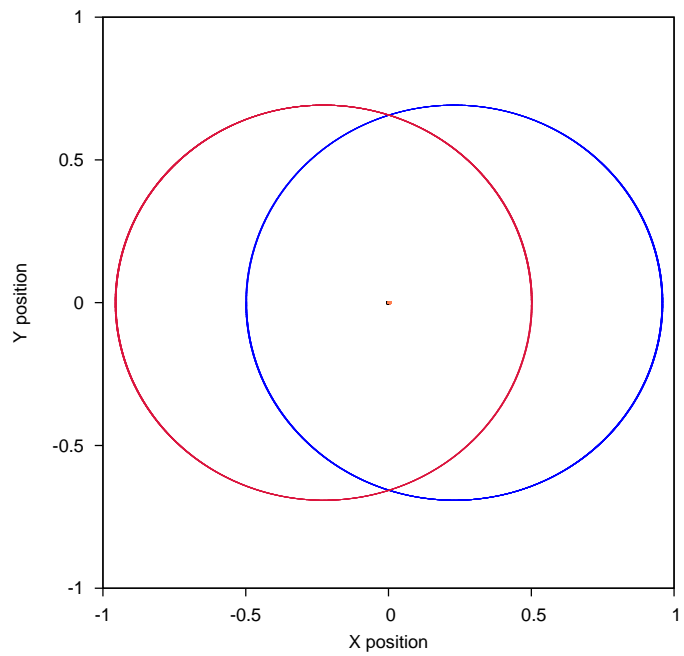


Figure 22: Configuration 10

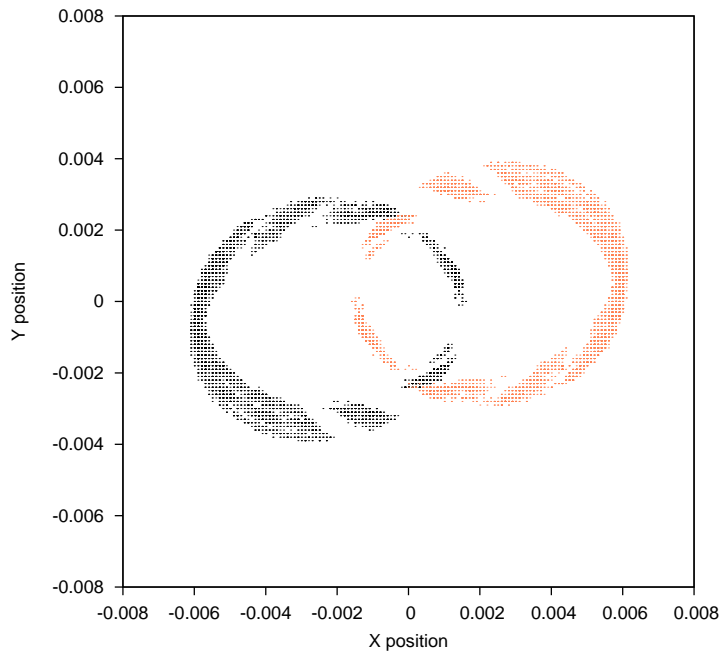


Figure 23: Configuration 10 - Inner Bar

In figs. 12 to 23 the initial velocity of the outer binary has also been gradually increased to also counteract the effect of the increased mass of the

inner binary. In order for these systems to be relatively stable the initial velocity of the inner binary was reduced. At this point both the inner and outer binaries had started to separate and become increasingly elliptical.

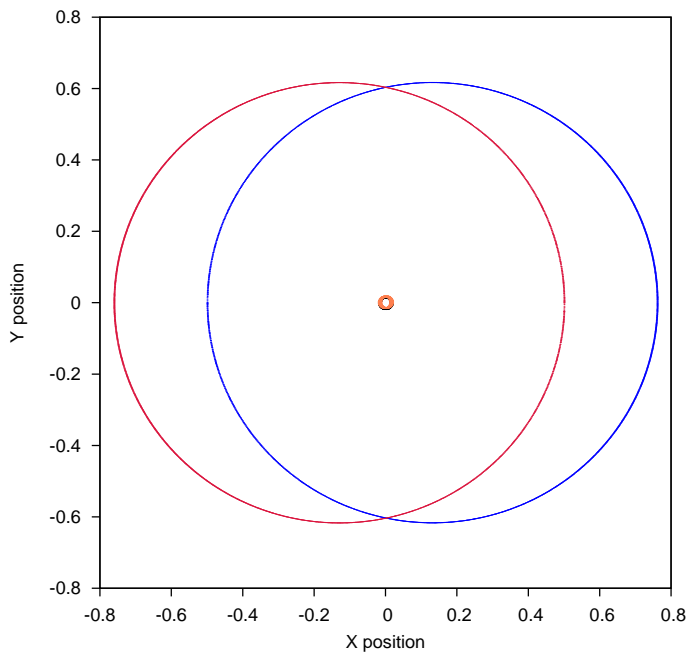


Figure 24: Configuration 11

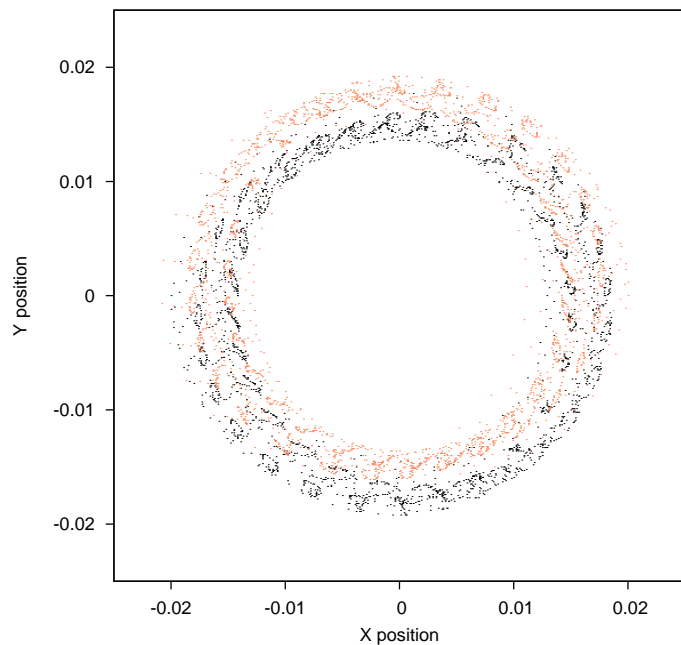


Figure 25: Configuration 11 - Inner Bar

In order to bring the orbits back into approximate circularity it was necessary to again increase the velocity of the inner binary. This is illustrated in Figs. 24 and 25. The mass of the inner binary has also increased considerably from the previous configurations.

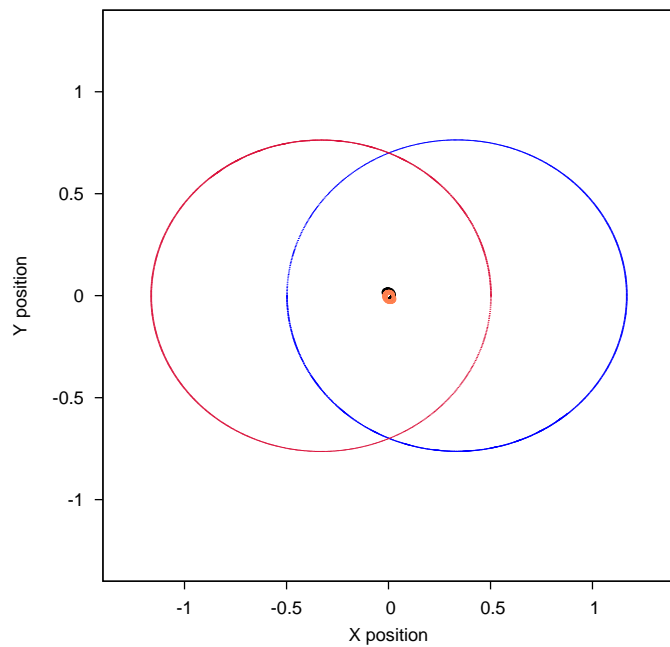


Figure 26: Configuration 12

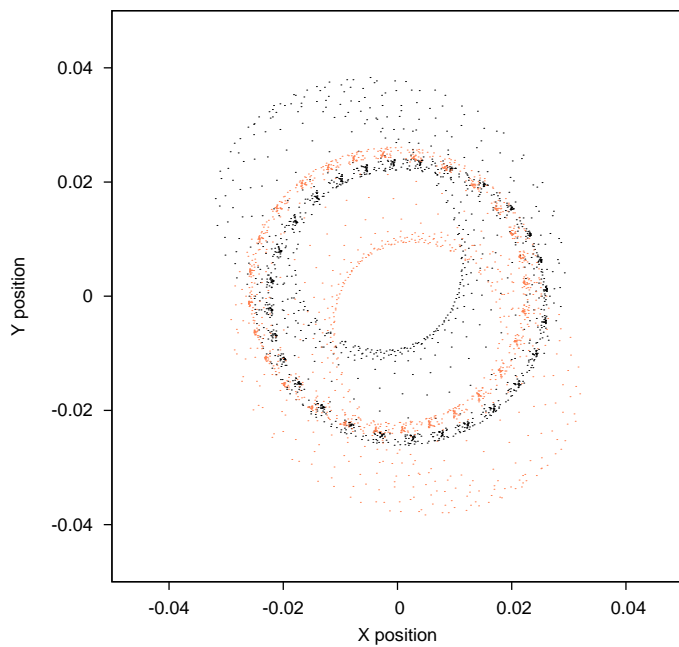


Figure 27: Configuration 12 - Inner Bar

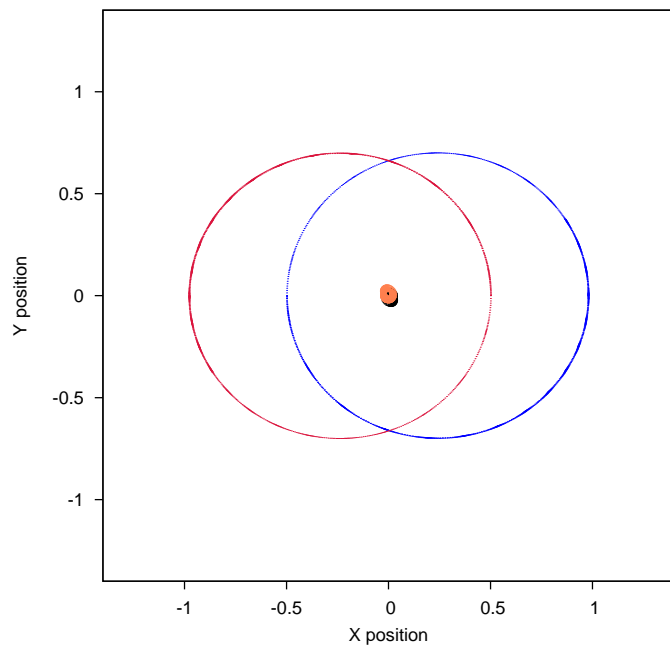


Figure 28: Configuration 13

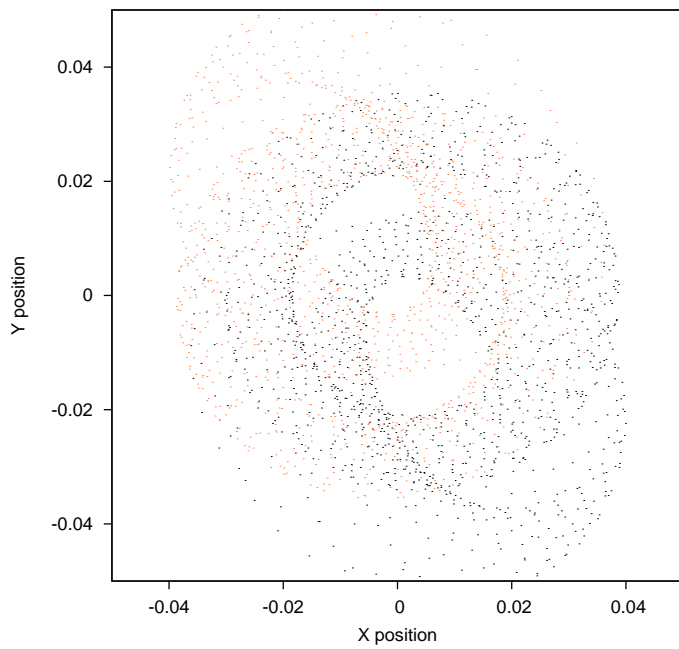


Figure 29: Configuration 13 - Inner Bar

Figs. 26 to 29 show the mass of the inner binary slowly increasing and adjustments made to both velocity of outer binary and separation of inner

binary.

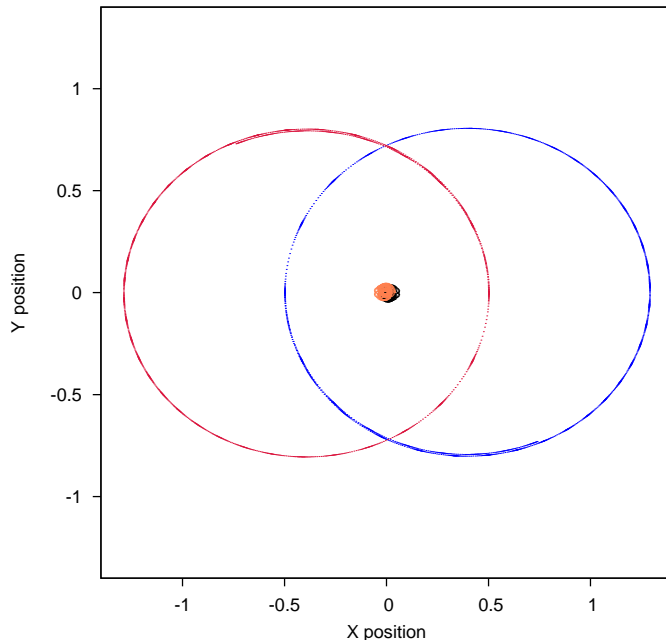


Figure 30: Configuration 14

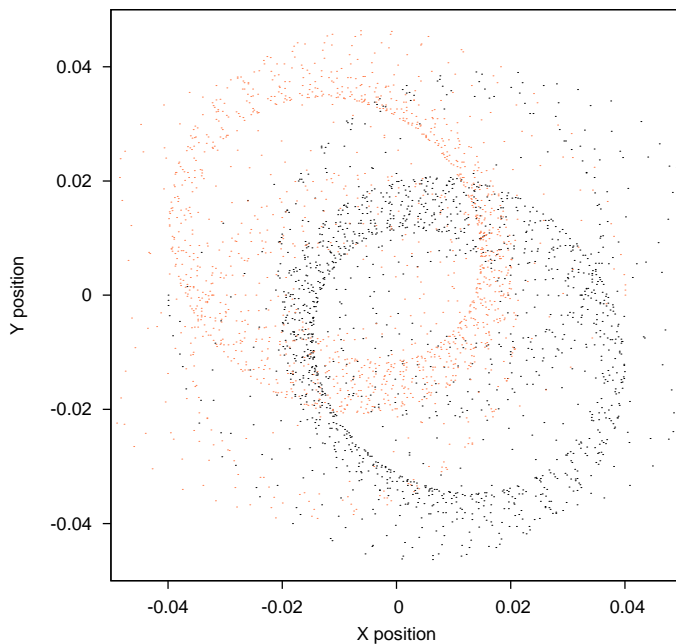


Figure 31: Configuration 14 - Inner Bar

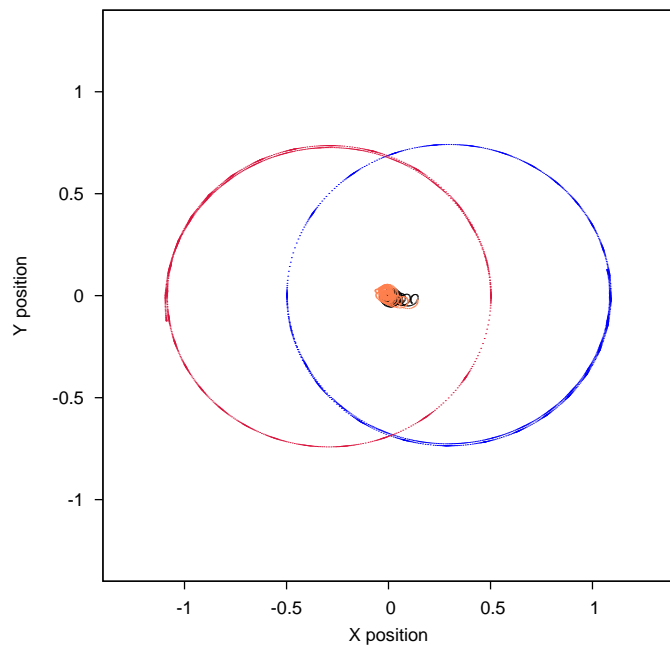


Figure 32: Configuration 15

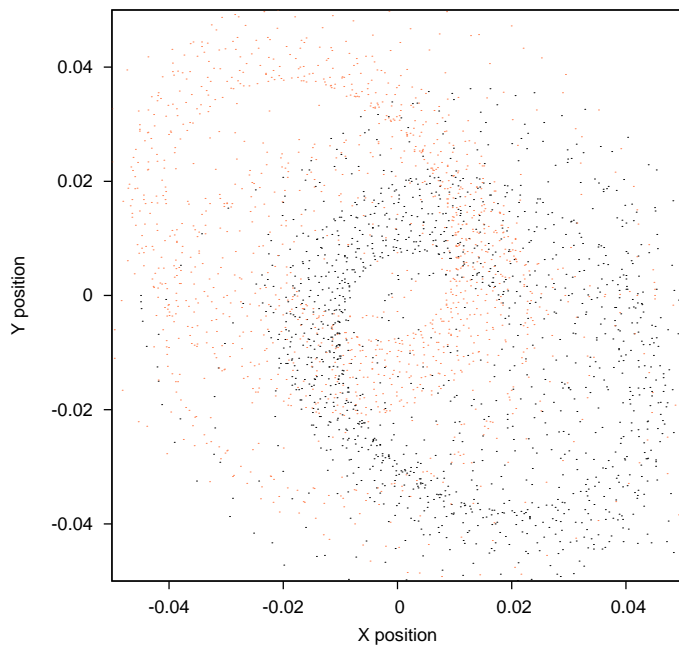


Figure 33: Configuration 15 - Inner Bar

As the mass of the inner binary was increased, it became necessary to reduce the velocity of the inner binary, Figs. 30 to 33.

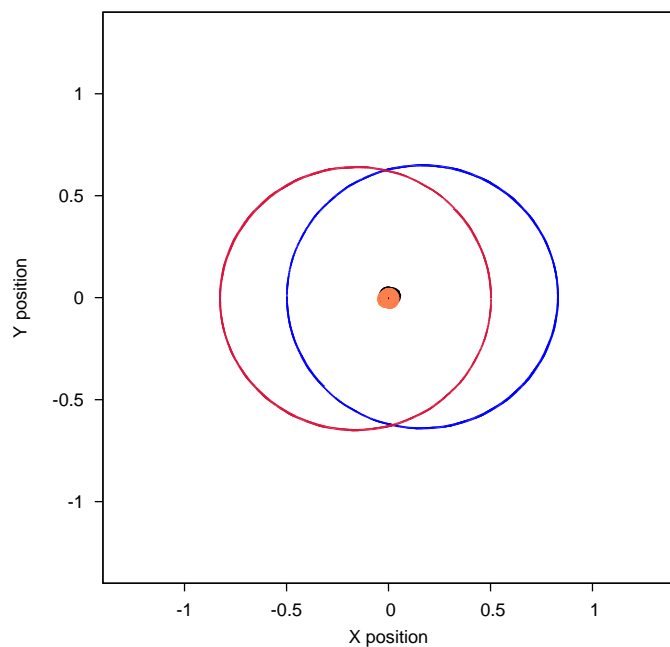


Figure 34: Configuration 16

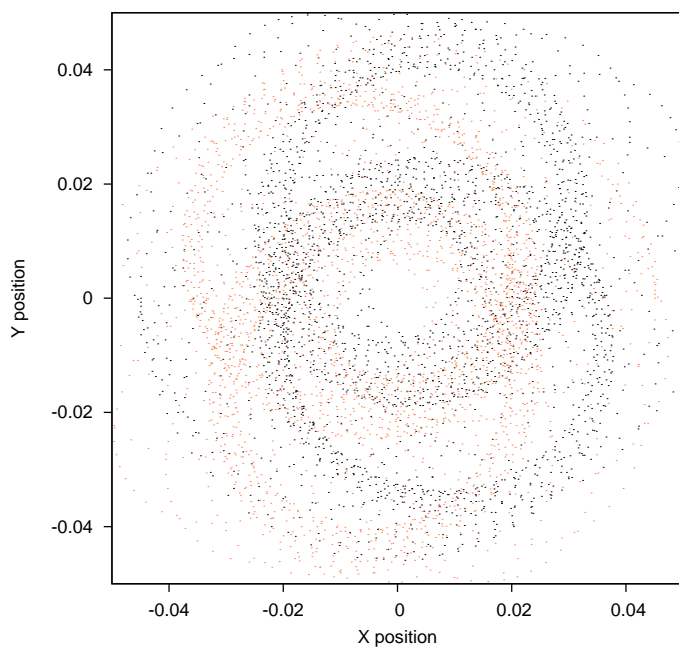


Figure 35: Configuration 16 - Inner Bar

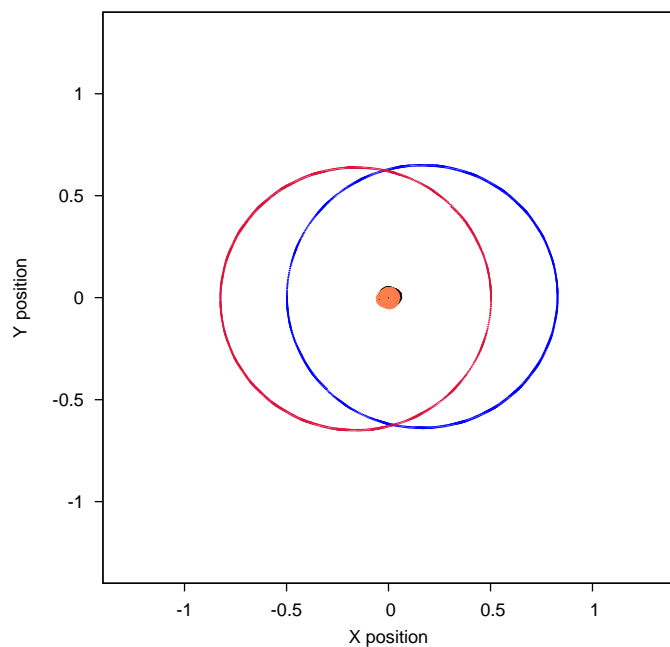


Figure 36: Configuration 17

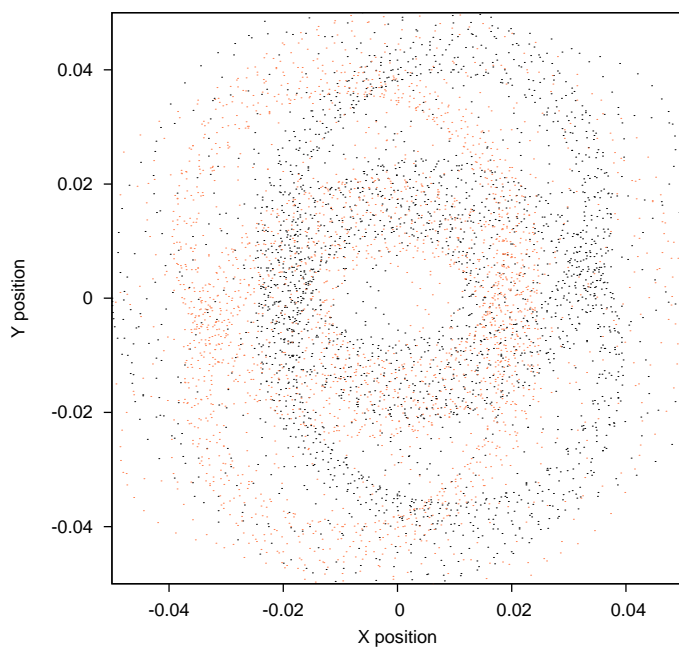


Figure 37: Configuration 17 - Inner Bar

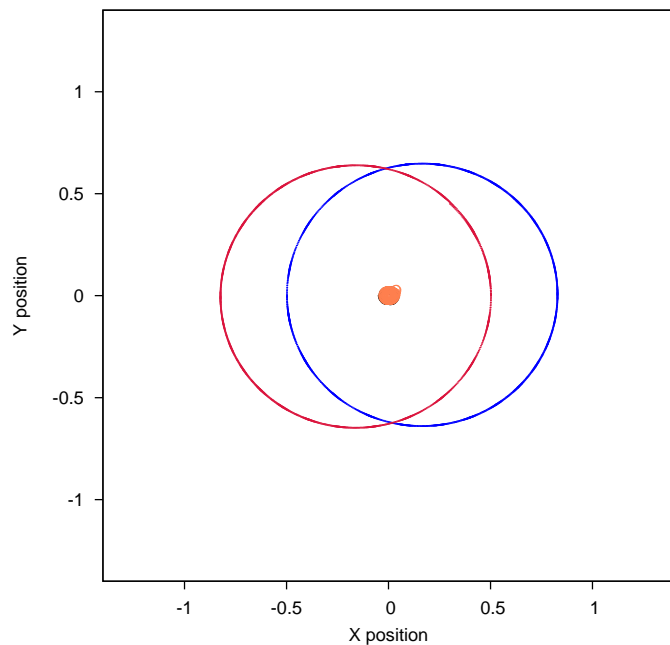


Figure 38: Configuration 18

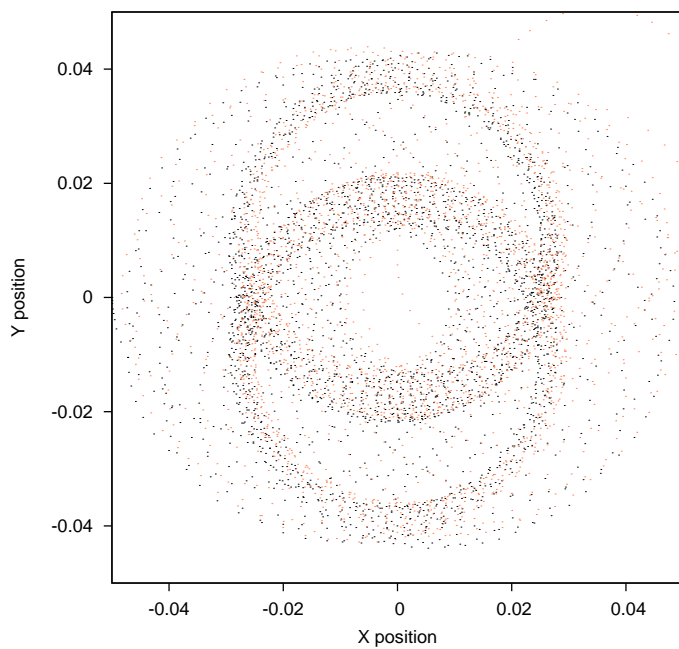


Figure 39: Configuration 18 - Inner Bar

Holding the mass of the inner binary at .05 the system showed signs of more stability if the velocity of the inner binary was further reduced, Figs.

34 to 39.

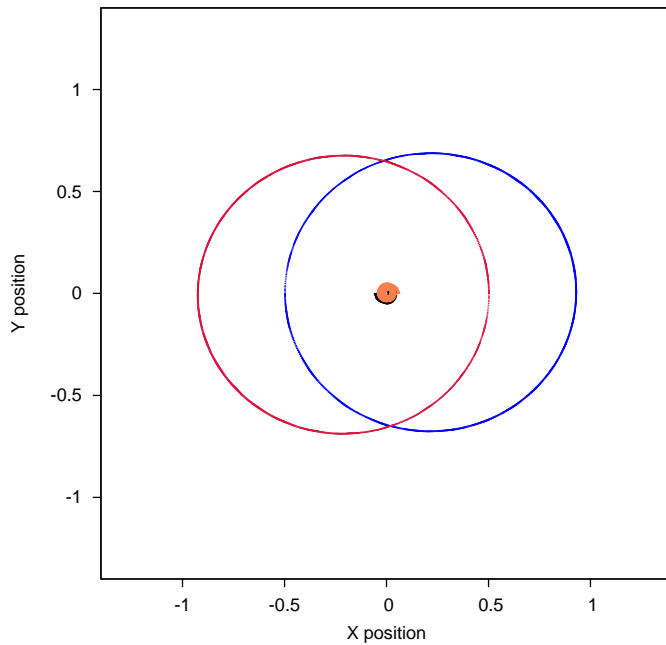


Figure 40: Configuration 19

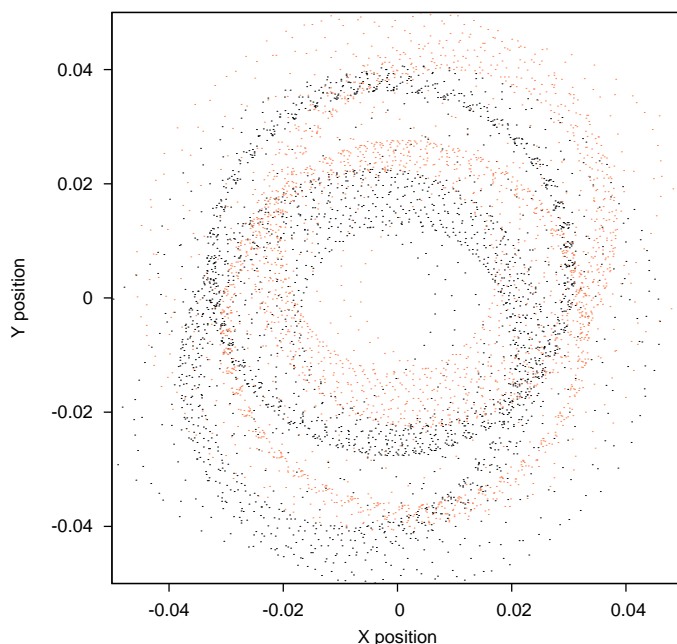


Figure 41: Configuration 19 - Inner Bar

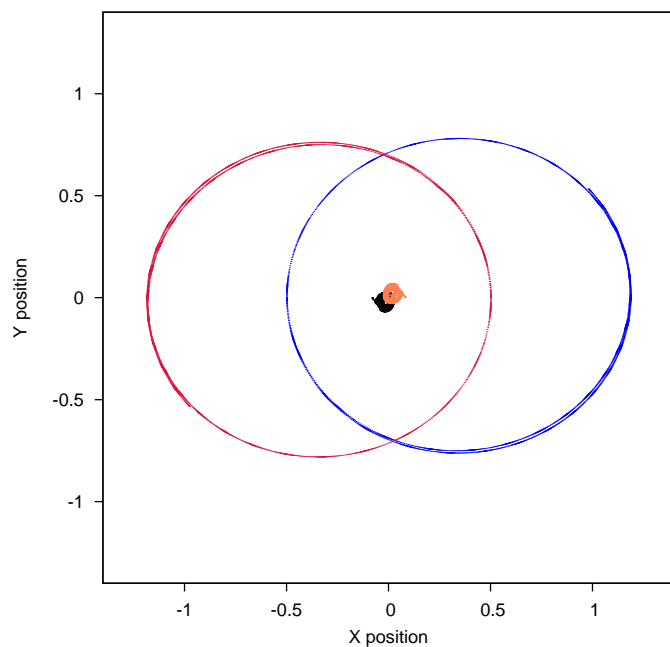


Figure 42: Configuration 20

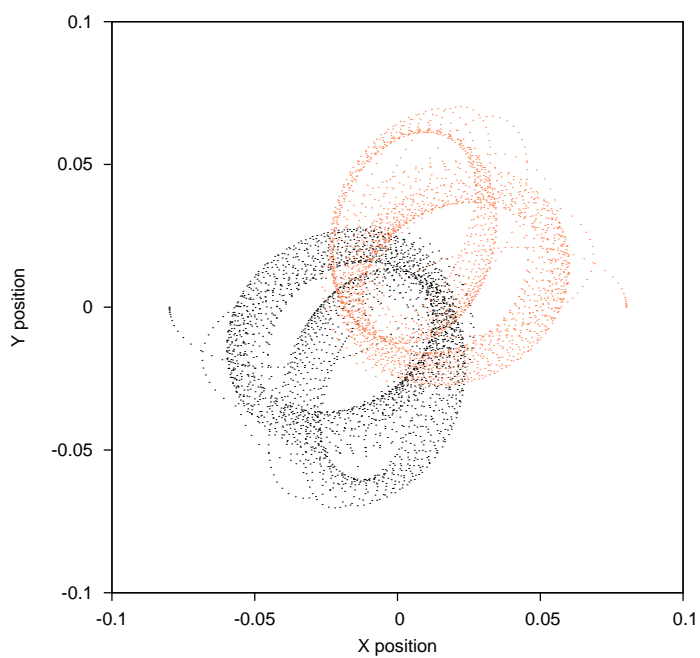


Figure 43: Configuration 20 - Inner Bar

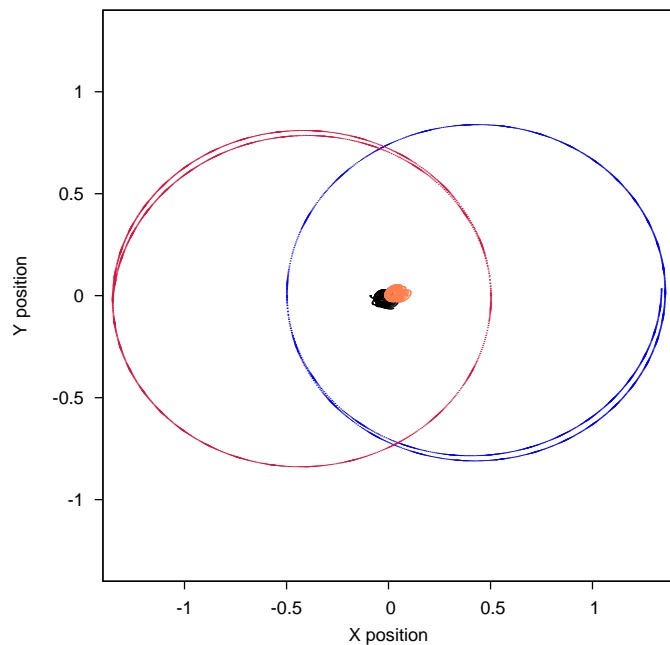


Figure 44: Configuration 21

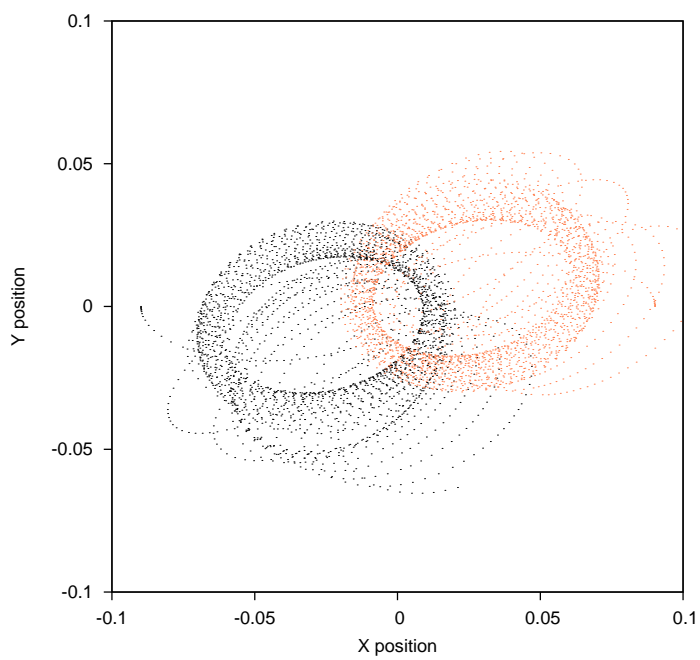


Figure 45: Configuration 21 - Inner Bar

Further reduction of the velocity of the inner binary allowed further increase of inner binary mass without losing stability, Figs. 40 to 45.

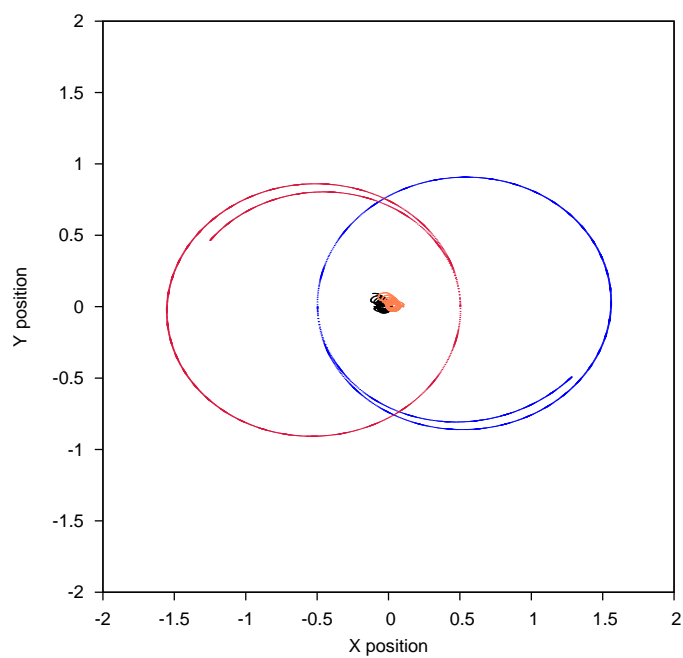


Figure 46: Configuration 22

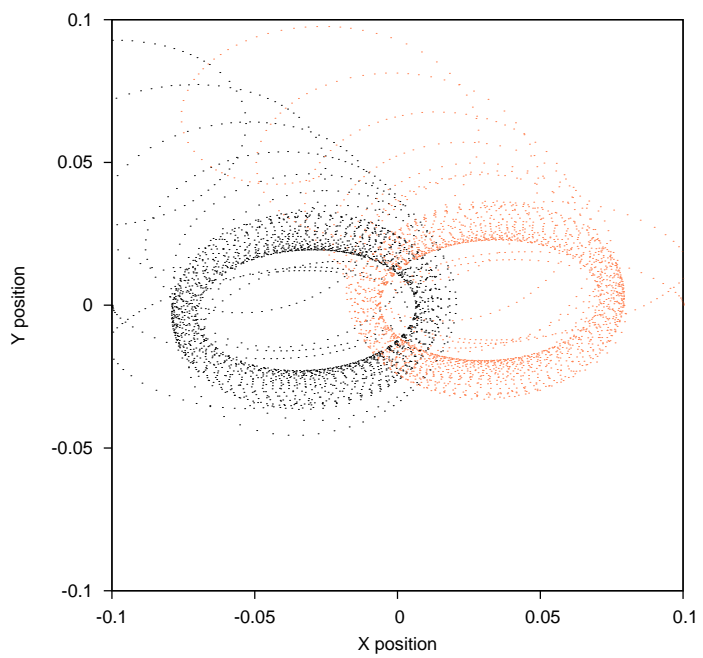


Figure 47: Configuration 22 - Inner Bar

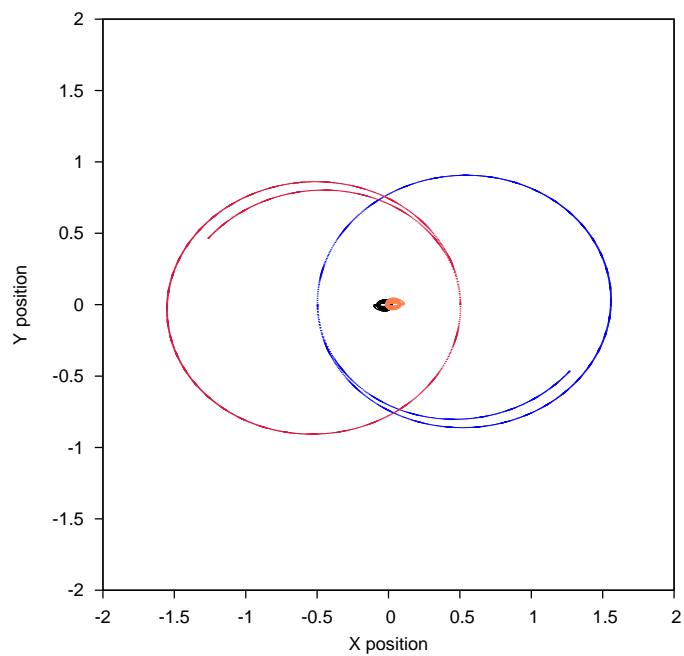


Figure 48: Configuration 23

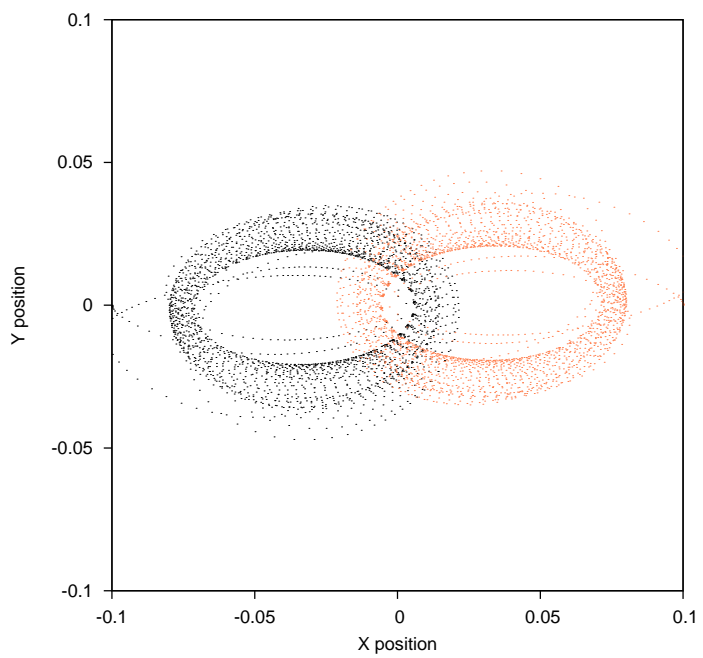


Figure 49: Configuration 23 - Inner Bar

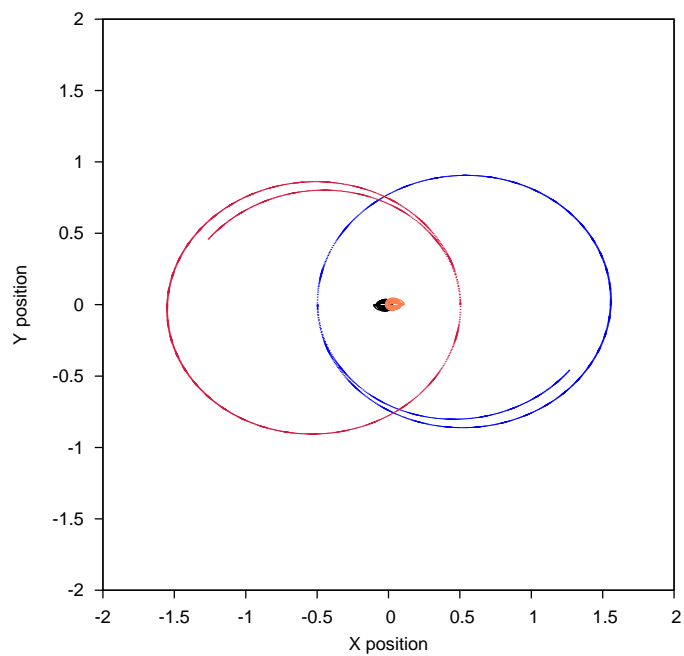


Figure 50: Configuration 24

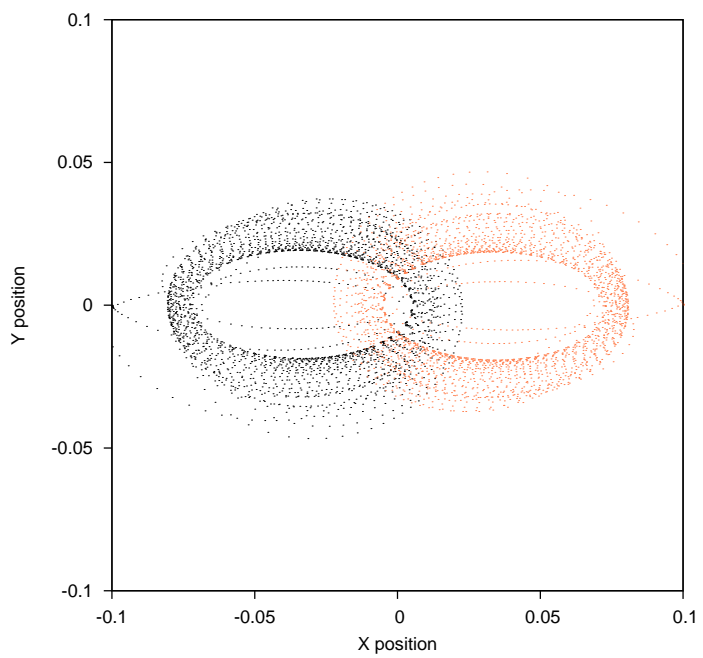


Figure 51: Configuration 24 - Inner Bar

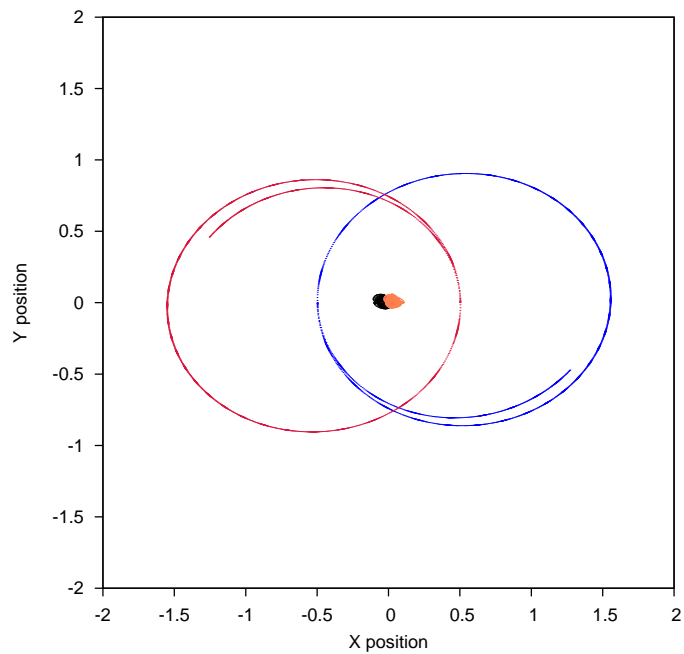


Figure 52: Configuration 25

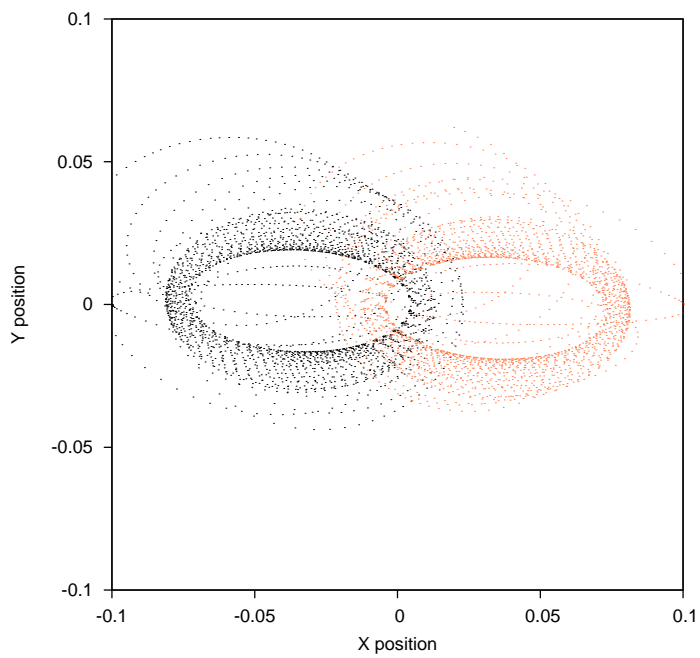


Figure 53: Configuration 25 - Inner Bar

With the mass of the inner binary now a quite considerable .1, the system showed more signs of stability if the velocity of the inner binary was further

reduced, Figs. 46 to 53.

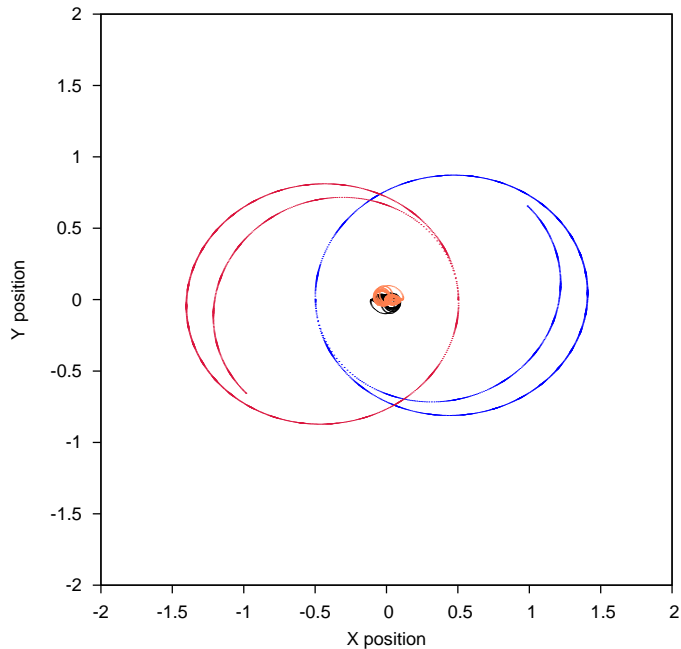


Figure 54: Configuration 26

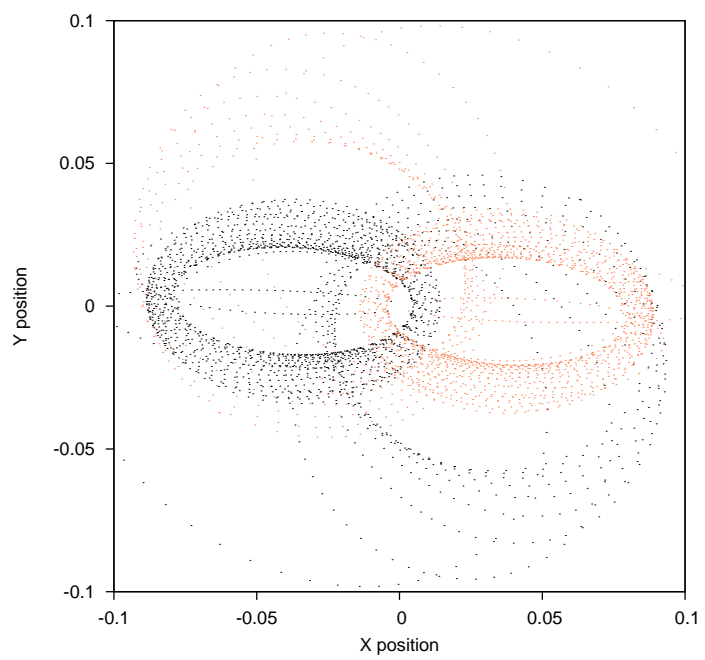


Figure 55: Configuration 26 - Inner Bar

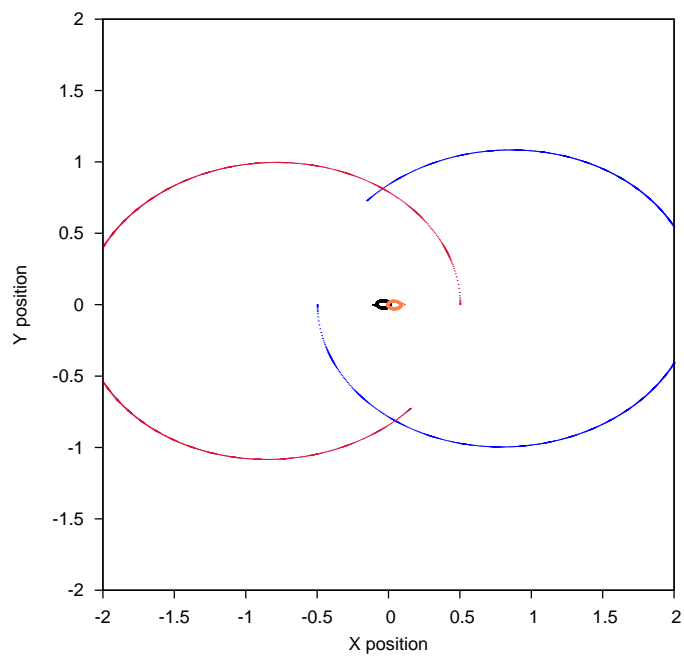


Figure 56: Configuration 27

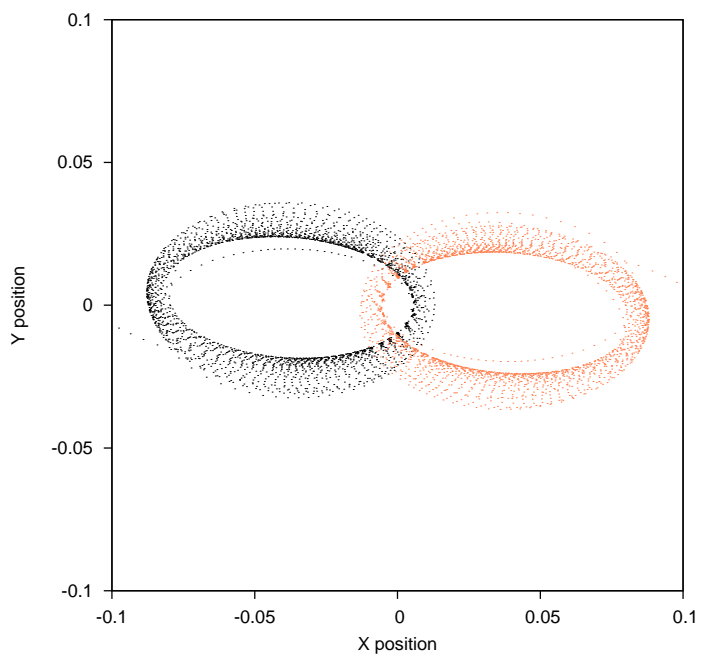


Figure 57: Configuration 27 - Inner Bar

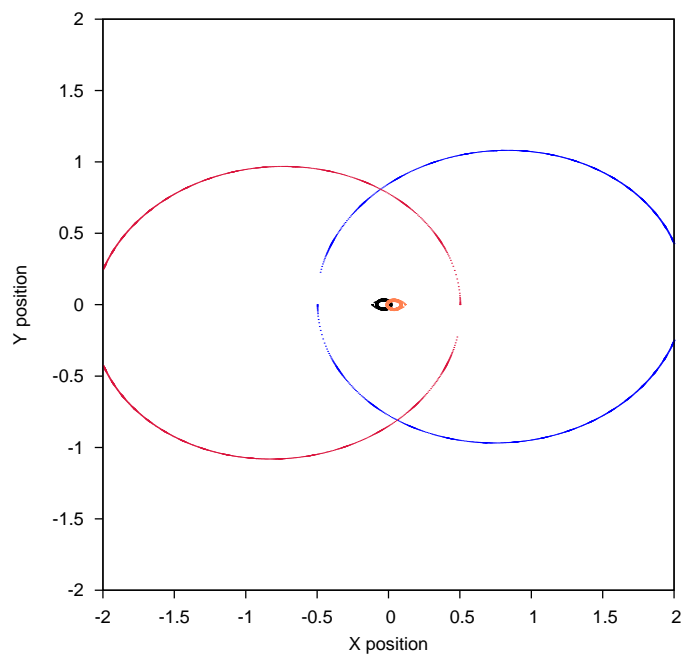


Figure 58: Configuration 28

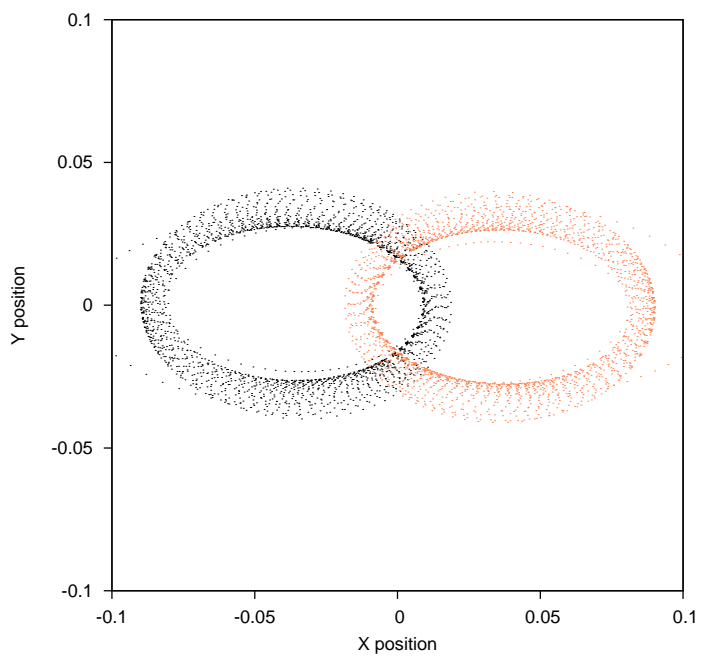


Figure 59: Configuration 28 - Inner Bar

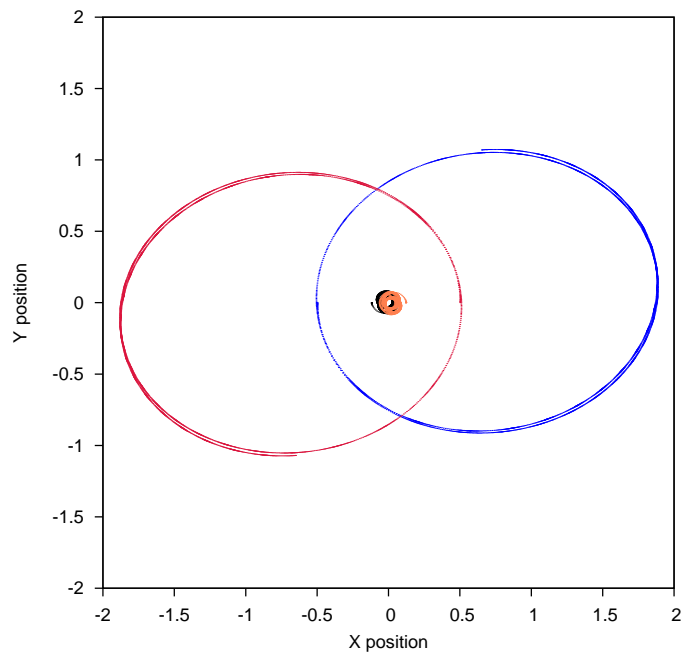


Figure 60: Configuration 29

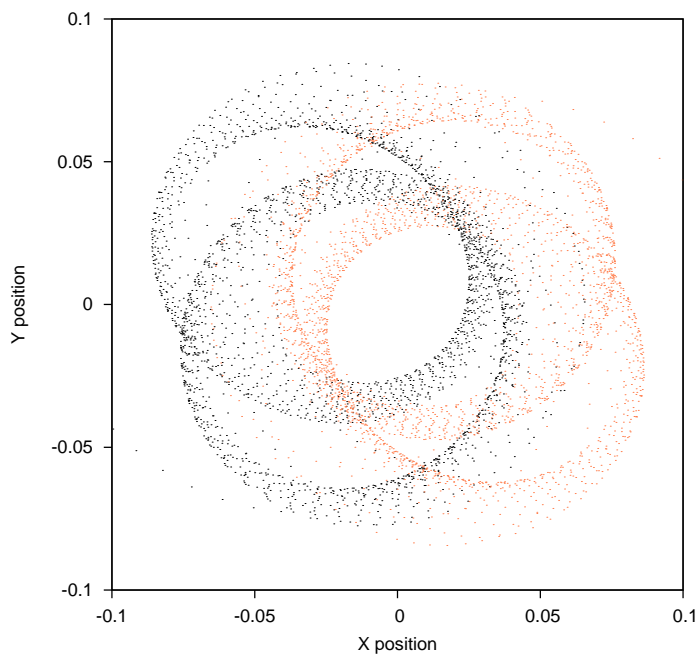


Figure 61: Configuration 29 - Inner Bar

In Figs. 54 to 61 the mass of the inner binary was increased to .12, and various adjustments made to inner separation, velocity and outer velocity to

maintain stability.

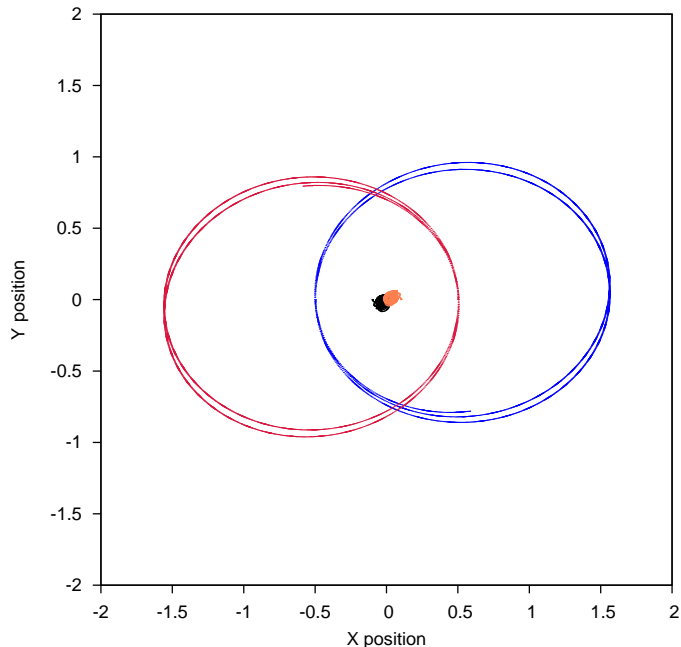


Figure 62: Configuration 30

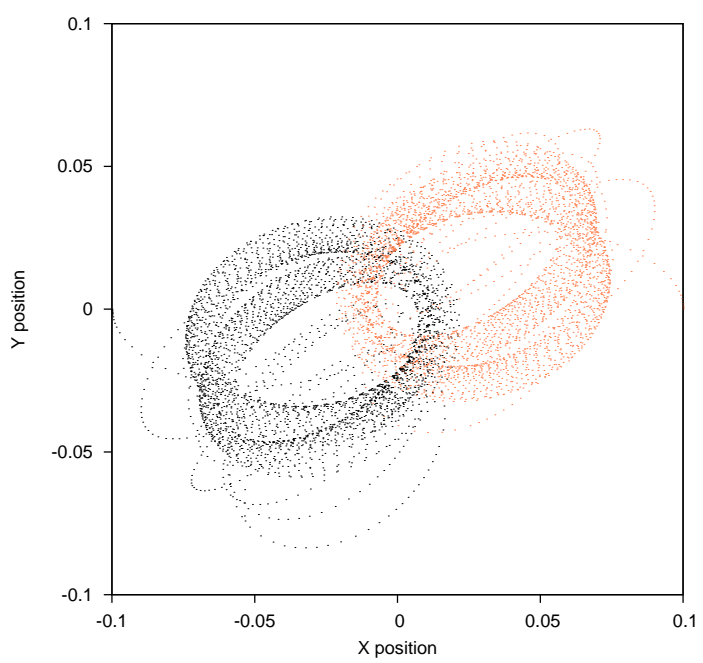


Figure 63: Configuration 30 - Inner Bar

Having increased the mass of the inner binary to .12 on the previous three plots it was decided, that as inner bars are generally $\approx 12\%$ of the mass of the outer bar, the mass of the inner binary could stay at .1 as this is 20% of the mass of the outer binary, Figs. 62 and 63.

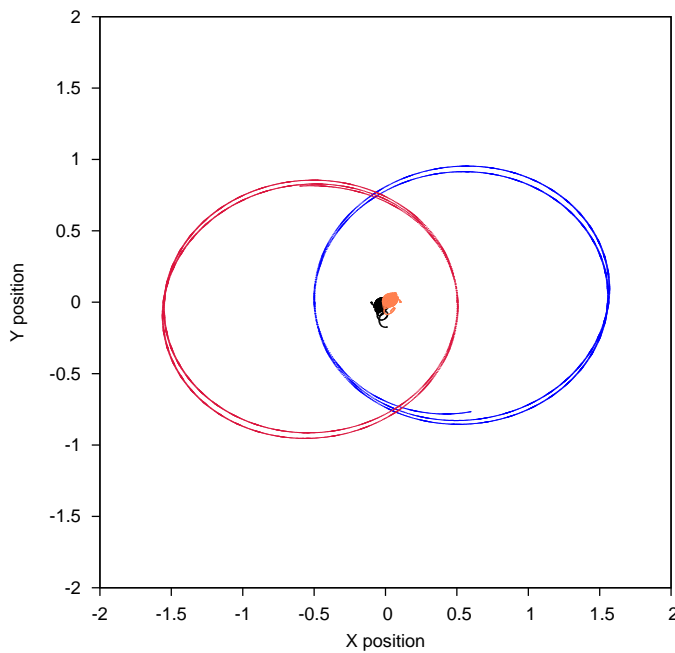


Figure 64: Configuration 31

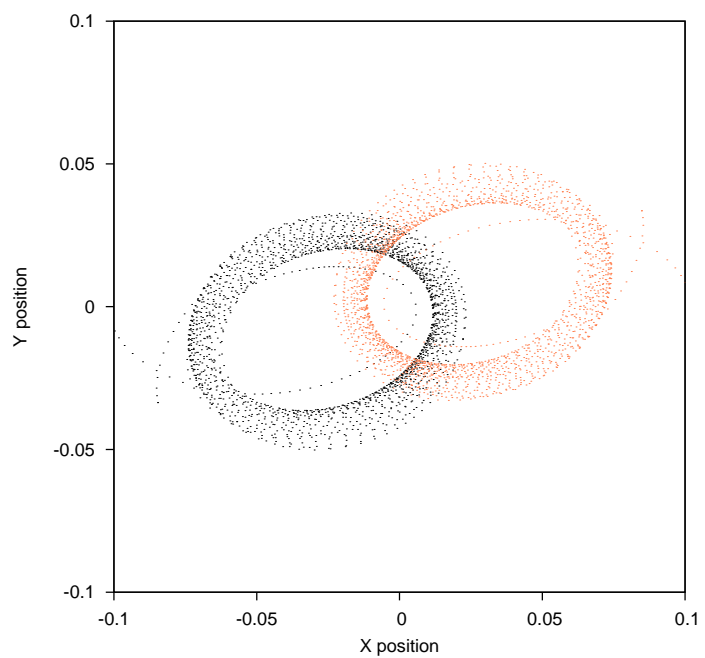


Figure 65: Configuration 31 - Inner Bar

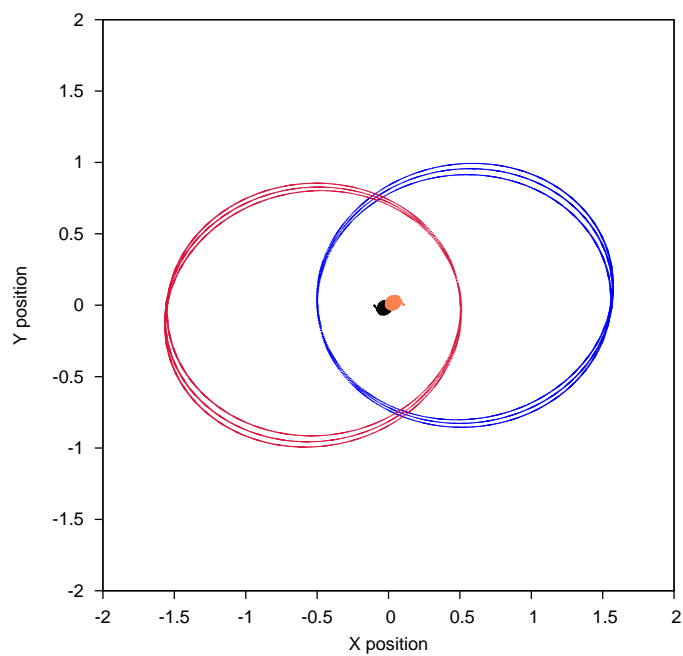


Figure 66: Configuration 32

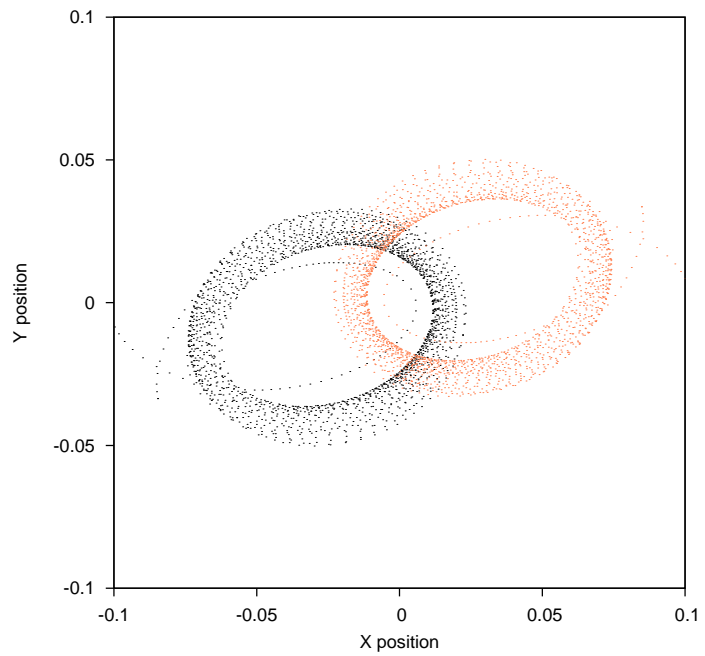


Figure 67: Configuration 32 - Inner Bar

Finally, Figs. 64 to 67 show the mass of the inner binary held at .1, but with minor adjustments made to the inner binary separation to enhance stability. The final plot was very stable and allowed the simulation to run for far longer than all the other runs. This may be a resonance, please see Discussion. Although this final system was very stable, even minor deviations from the initial conditions immediately resulted in destabilisation of the system, and chaos.

4 Discussion

The final three runs (configurations 30, 31, and 32) were by far the most stable. The orbital periods vary slightly with time so it is difficult to give accurate figures, so the periods of the first orbit were used to calculate the ratio of the periods between inner and outer binaries. The following table shows the periods of the two binaries together with the ratios of the corresponding periods.

Table 2: Periods

Config.	Inner	Outer	Ratio	Length of simulation
30	.51	11.56	1:22.7	25
31	.54	11.5	1:21.3	25
32	.55	11.5	1:20.9	35

Configuration 32 was by far the longest running simulation showing almost three complete orbits of the outer binary and many orbits of the inner binary. It showed no signs of destabilising and the simulation only ended because of a 'Step size underflow' in the integrator. This error occurs when the adaptive stepsize becomes too small and the integrator is effectively not making any progress with the integration and so ends the simulation. The data shows that as the periodic ratios tends towards 1:21 the system considerably stabilises. 1:21 could therefore possibly be an orbital resonance. Attempts at modifying the initial conditions of configuration 32 even slightly resulted in chaotic systems.

Unfortunately a 1:21 resonance doesn't represent the observational data of double-barred galaxies. Font el. al. (2014) found that the inner bar rotates more rapidly than the outer bar by a factor between 3.3 and 3.6. Whilst Maciejewski and Athanassoula (2008) predicted values for the ratio of bar angular rates between 1.6 and 2.7.

4.1 Future Work

As this system has a multi-dimensional parameter space, finding stable configurations was very time consuming. I suggest further studies in this area try to automate this process. It may be possible for an automated process to automatically reject systems in which there are collisions, or if any of the bodies exits the system, or if the system fails to persist for a certain number of orbits. In this way it may be possible to find further orbital resonances.

References

- Aarseth, S., Gravitational N-Body Simulations, 2003, Cambridge University Press
- AlvarezRamirez, M., Medina, M., A Review of the Planar Caledonian Four-Body Problem, 2014
- Binney, J., Tremaine, S., Galactic Dynamics, 2008, Princeton University Press
- de Vaucouleurs, G., 1975, ApJS, 29, 193
- Debattista, V., Shen, J., Long-Lived Double-Barred Galaxies from Pseudobulges, 2007, The Astrophysical Journal, 654: L127L130, 2007 January 10
- Du, M., Shen, J., Debattista, V., Forming Double-Barred Galaxies from Dynamically Cool Inner Disks, 2015, The Astrophysical Journal, 804:139 (10pp), 2015 May 10
- Erwin, P., Double-Barred Galaxies I. A Catalog of Barred Galaxies with Stellar Secondary Bars and Inner Disks, 2003, arXiv:astro-ph/0310806v2
- Erwin, P., Double-Barred Galaxies, 2011, Mem. S.A.It. Suppl. Vol. 18, 145
- Erwin, P., Sparke, L., Double Bars, Inner Disks, and Nuclear Rings in Early-Type Disk Galaxies, 2002, The Astronomical Journal, 124:6577, 2002 July
- Font, J., Beckman, J., E., Zaragoza-Cardiel, J., Fathi, K., Epinat, B., Amram, P., The ratio of pattern speeds in double-barred galaxies, arXiv:1408.4274v1
- Garzon, F., Lopez-Corredoira, M., Dynamical evolution of two associated galactic bars, 2014, arXiv:1409.1916.v1
- Heggie D., Hut, P., The Gravitational Million-Body Problem, 2003, Cambridge University Press
- de Lorenzo-Caceres, A., Vazdekis, A., Aguerri, K., A., L., Corsini, E., M., Debattista, V., P., Constraining the formation of inner bars. Photometry, kinematics and stellar populations in NGC357, 2002, arXiv:1111.1718v1
- de Lorenzo-Caceres, A., Falcon-Barroso, J., Vazdekis, A., Distinct stellar populations in the inner bars of double-barred galaxies, 2013, arXiv:1302.5701v1

- Maciejewski, W., Teuben, P., J., Sparke, L., S., Stone, J., M., Gas Inflow in Barred Galaxies - Effects of Secondary Bars, arXiv:astro-ph/0109431v1
- Maciejewski, W., Orbits in corotating and counterrotating double bars, 2008, arXiv:0801.1471v1
- Maciejewski, W., Athanassoula, A., Regular motions in double bars. II. Survey of trajectories and 23 models, 2008, arXiv:0805.3967v1
- Maciejewski, W., Small, E., Orbital Support of Fast and Slow Inner Bars in Double Barred Galaxies, 2010, arXiv:1006.4574v1
- Maciejewski, W., Sparke, L., Bars within Bars in Galaxies, 1998, arXiv:astro-ph/9812228v1
- Maciejewski, W., Sparke, L., Orbits Supporting Bars within Bars, 1999, arXiv:astro-ph/9911281v1
- Malhotra, R., Orbital Resonances and Chaos in the Solar System, 1998, Solar system Formation and Evolution ASP Conference Series, Vol. 149, 1998
- Manos, T., Athanassoula, E., Regular and chaotic orbits in barred galaxies - I. Applying the SALI/GALI method to explore their distribution in several models, 2011, arXiv:1102.1157v2
- Moiseev, A., V., Velocity dispersion of stars and gas motion in double-barred galaxies, 2001, arXiv:astro-ph/0111220v1
- Press, W., H., Teukolsky, S., A., Vetterling, W., T., Flannery, B., P., Numerical Recipes in Fortran 77 The Art of Scientific Computing, 2nd edition
- Saha, K., Maciejewski, W., Spontaneous formation of double bars in dark matter dominated galaxies, 2013, arXiv:1304.7108v1
- Shen, J., Debattista, V., Long-lived double-barred galaxies in N-body simulations, 2008, Mem. S.A.It. Vol. 00, 169
- Shen, J., Debattista, V., Observable Properties of Double-Barred Galaxies in N-Body Simulations, 2009, The Astrophysical Journal, 690:758772, 2009 January 1
- Shlosman, I., Frank, J., Begeman, M.,C., 1989, Nature, 338, 45
- Steves, B., Roy, A., Some special restricted four-body problems-I. Modelling the Caledonian problem, 1998, Phrt. Spucx, Si., Vol. 46. No. I I /) 12, pp. 1465-1474, 1998

Szell, A., Erdi, B., Sandor, Zs., Steves, B., Chaotic and stable behaviour in the Caledonian Symmetric Four-Body Problem, 2004, Mon. Not. R. Astron. Soc. 347, 380388 (2004)

Trenti, M., Hut, P., Gravitational N-body Simulations, 2008, arXiv:0806.3950v1

Wozniak, H., How can double-barred galaxies be long-lived?, 2015, A and A 575, A7 (2015)